Behavioral/Cognitive

Probability-Dependent Scaling of Fear Responding, But Not Unconditioned Stimulus Inflation, Requires the Periaqueductal Gray

Liliuokalani H. Counsman, Genevieve E. Valvo, Courtney F. Lamberson, Aleah M. DuBois, Ziling Vicky Lyu, Hoyeon Esther Kim, Tatum Suyeong Lee, Maya J. Garcia-Viesca, Jacob B. Boyce, Selena M. Shen, Anaise C. Fitzpatrick, Madeline L. David, Mahsa Moaddab, and Michael A. McDannald*

Department of Psychology & Neuroscience, Boston College, Chestnut Hill, Massachusetts 02467

Adaptive behavior requires animals to estimate threat, update these estimates following new aversive experiences, and align fear responding to up-to-date estimates. The periaqueductal gray (PAG) is traditionally viewed as a downstream relay that converts threat estimates into freezing. Here we tested whether the PAG is necessary for probability-dependent scaling of fear responding and for updating threat estimates through unconditioned stimulus inflation. We deleted neurons across the complete anterior–posterior span of the PAG using a dual-viral approach and then quantified deletion extent and subregion specificity using machine-learning methods. In Experiment 1, 40 Long–Evans rats (20 females) underwent fear discrimination in which a threat cue predicted footshock with 30 or 10% probability, while a neutral cue never predicted footshock. Ethograms revealed that control rats scaled a suite of reward, exploratory, and defensive behaviors to threat probability (threat > neutral and 30 > 10%). PAG deletion abolished scaling (threat > neutral, but 30 ≈ 10%). In Experiment 2, 40 Long–Evans rats (20 females) first received separate light conditioning and tone conditioning with a mild footshock. During unconditioned stimulus inflation, half the rats received light–intense shock pairings, while the other half received additional light–mild shock pairings. PAG deletion left inferred inflation intact (intense > mild; tone extinction responding) and enhanced direct inflation (intense > mild; light extinction responding). These results demonstrate that the PAG is essential for scaling fear responding to threat probability, but dispensable for, and can even constrain, updating threat predictions through unconditioned stimulus inflation.

Key words: **associative; fear; freezing; periaqueductal; threat; uncertainty**

Significance Statement

This important work demonstrates the essential role of the periaqueductal gray (PAG), widely considered to simply organize freezing, in scaling behavior systems-level responding to threat probability. The evidence supporting these conclusions is compelling, including the use of innovative probabilistic fear discrimination and unconditioned stimulus inflation procedures, machine learning-based quantification of neuronal deletion, comprehensive ethograms, and bidirectional analyses linking PAG deletion to probability-insensitive fear responding. These results identify the PAG as a critical site where disruption of threat estimation may contribute to stress and anxiety disorders.

Introduction

Real-world threats are rarely absolute but are instead uncertain. Appropriate threat responding requires scaling fear to an accurate probability estimate. A dynamic world requires threat predictions to be updated in light of new aversive experiences. A core threat circuit consisting of the amygdala and periaqueductal gray (PAG) has been established. Within this core circuit, the lateral, basal, and central amygdala nuclei are viewed as mediating threat learning and prediction (LeDoux et al., 1990; Davis, 1992; Fanselow and Kim, 1994; Maren, 1999; Goosens and Maren, 2001; Choi and Brown, 2003; Koo et al., 2004; Lee et al., 2005; Wilensky et al., 2006; Ciocchi et al., 2010; McDannald, 2010; Li et al., 2013; Liu et al., 2022). The PAG is widely viewed as mediating freezing (Kim et al., 1993; Fanselow et al., 1995; De Oca et al., 1998; McDannald, 2010; Assareh et al., 2016; Vaaga et al., 2020; Signoret-Genest et al., 2023), one of the most commonly studied fear conditioned

Received Jan. 6, 2026; revised Sept. 8, 2026; accepted Sept. 12, 2026.

Author contributions: L.H.C., G.E.V., and M.A.M. designed research; L.H.C., G.E.V., C.F.L., A.M.D., Z.V.L., H.E.K., T.S.L., M.J.G-V., J.B.B., S.M.S., A.C.F., M.L.D., and M.A.M. performed research; H.E.K. contributed unpublished reagents/analytic tools; L.H.C., G.E.V., C.F.L., A.M.D., T.S.L., M.J.G-V., M.M., and M.A.M. analyzed data.

The authors declare no competing financial interests.

This work was supported by National Institutes of Health (NIH), R01-MH117791.

*M.A.M is the lead contact.

Correspondence should be addressed to Michael A. McDannald at michael.mcdannald@bc.edu.

This paper contains supplemental material available at: https://doi.org/10.1523/JNEUROSCI.0041-26.2026

https://doi.org/10.1523/JNEUROSCI.0041-26.2026

Copyright © 2026 the authors

behaviors (McDannald, 2023). Yet, the PAG plays roles in threat beyond freezing. Prediction errors generated by the PAG modulate associative strength and behavioral responding to shock-predictive cues (Ozawa et al., 2017; Walker et al., 2019). Newer evidence supports a role in signaling threat prediction. In rats undergoing probabilistic fear discrimination, PAG neurons rapidly scale cue firing to shock probability (Wright and McDannald, 2019). High-density recordings further reveal the PAG as a hub for brainstem threat probability signaling (Strickland and McDannald, 2022).

Two experiments set out to determine PAG roles in using and updating threat predictions. Both experiments utilized a dual-viral approach, consisting of local Cre insertion (Tervo et al., 2016) and Cre-dependent neuronal deletion (Yang et al., 2013) to delete neurons across the entire anterior–posterior extent of the PAG. Experiment 1 examined a PAG role in probability-dependent scaling of fear responding (Rescorla, 1968). Control and PAG-deleted rats received fear discrimination in which a threat cue was probabilistically paired with footshock (30 or 10%), while a neutral cue was not. Prior work from our laboratory found probability-sensitive threat responding. Specifically, while both threat cues supported greater fear responding than the neutral cue, the 30% threat cue supported greater responding than the 10% cue (30% > 10% > neutral; Russell and McDannald, 2024). Experiment 2 examined roles of the PAG in updating threat predictions. We drew from unconditioned stimulus inflation (Rescorla, 1974), in which subjects acquire fear to a cue predictive of mild shock and then increase fear following intense shock experience. We developed a novel unconditioned stimulus inflation procedure assessing updating through both inference and direct experience. Rats first received separate tone pairings and light pairings with mild footshock. Half the rats then received light pairings with intense footshock, while the other half received additional mild pairings. Inferred inflation was assessed via extinction responding to the tone, which was never paired with intense shock. Direct inflation was assessed via extinction responding to the light.

Two challenges to manipulating the PAG are its long anterior-posterior extent and its subregion organization. To overcome these challenges, both experiments used a dual-viral approach for deletion across the complete extent, paired with machine learning-based quantification by subregion (Berg et al., 2019). To more fully reveal the behavioral basis of threat responding, both experiments used comprehensive, subsecond ethograms (Chu et al., 2024; Williams et al., 2025). Comparing results across experiments would then distinguish several possible roles of the PAG. A deficit in probability-dependent scaling, but no deficit in inflation, would indicate a role specific to aligning fear behavior with a probability prediction. Dual deficits in probability-dependent scaling and inflation would indicate either a broader role in forming and updating threat predictions or a more basic role in processing footshock. A deficit restricted to freezing would reinforce the PAG's long-established role in organizing this single behavior, independent of the broader questions of scaling and updating.

Materials and Methods

Subjects

Experiment 1. Subjects were 40 Long–Evans rats (20 females) arriving from Charles River Laboratories on Postnatal Day (P)55, weighing 196–298 g. Upon arrival, rats were single housed and placed on a 12 h light cycle (lights off at 6:00 P.M.). Rats acclimated to the facility with *ad libitum* access to water and chow (18% Protein Rodent Diet 2018, Harlan Teklad Global Diets) for at least 2 weeks before behavioral testing or surgery.

Experiment 2. Subjects were 40 Long–Evans rats (20 females). Half (10 females) were from Charles River Laboratories and arrived at P55. The other half (10 females) were bred by pairing 1 male with 1–3 wild-type female(s) for 8–11 d. They were given *ad libitum* access to standard laboratory chow for the duration of pairing. After separation, all rats were singly housed, and the males had continued *ad libitum* access to standard chow, while the females received *ad libitum* access to an enriched breeding chow. Females also received straw and cotton nesting materials. Water was available *ad libitum* during pairing and in home cages before and after pairing. For litters with visible runts, pups were provided with a gelatinous saline solution for hydration with crushed standard chow strewn on top. Pups were weaned after 19−24 d and housed 2–3 per cage by sex. All rats were single housed after reaching adulthood. Charles River Laboratories rats acclimated to the facility with *ad libitum* access to water and chow (18% Protein Rodent Diet 2018, Harlan Teklad Global Diets) for at least 2 weeks before surgery and behavioral testing. All experiments were performed in accordance with the NIH guidelines regarding the care and use of rats for experimental procedures. All experiments were performed under Boston College IACUC Protocol #2024-001.

Surgery

Experiments 1 and 2. Aseptic, stereotaxic surgery was performed under isoflurane anesthesia (1–5% in room air). Carprofen (5 mg/kg, s.c.), lactated ringer's solution (5 ml, s.c.), and 2% lidocaine (~1.5 ml, s.c.) were administered preoperatively. The cranium was exposed via midline incision. Four holes were drilled above the PAG: AP −7.10 mm and ML ±1.42 mm and AP −8.00 mm and ML ±1.60 mm. At each site, PAG deletion (PAGd) rats received a 0.5 µl infusion of a 50/50 mixture of AAV2-eSyn-EGFP-T2A-iCre-WPRE + AAV-flex-taCasp3-TEVp. At each site, Control rats received a 0.5 infusion of a 40/60 mixture of AAV2-eSyn-EGFP-T2A-iCre-WPRE + saline. The syringe was lowered at a 10° angle toward the midline for each site. The DV for the anterior infusions was −5.89 mm, and the DV for the posterior infusions was −6.04 mm. Infusions were delivered via 2 µl syringes (Hamilton, Neuros) controlled by a microsyringe pump (World Precision Instruments, UMP3-2). The syringe was left in place for 5 min before the infusion. After the infusion, there was a 30 s wait, 0.1 mm raise, 2 min wait, 0.1 mm raise, and then a 4.5 min wait before syringe removal. This procedure was used to encourage viral delivery to the target site. Syringes were rinsed with saline between infusions. The dual-viral approach meant brainstem PAG neurons would be deleted in Caspase-3 rats but left intact in Control rats.

Postoperative procedures

Rats received Rimadyl (Bio-Serv MD150-2, 2 mg/tablet) for postoperative analgesia for 2 d postsurgery. At least 4 weeks passed between surgery and footshock sessions to permit caspase-3-mediated neuronal deletion.

Behavior apparatus

The behavior apparatus consisted of eight individual chambers with aluminum front and back walls, clear acrylic sides and top, and a grid floor. LED strips emitting 940 nm light were affixed to the acrylic top to constantly illuminate the behavioral chamber for frame capture. Illumination at 940 nm was chosen because rats do not detect light wavelengths exceeding 930 nm (Nikbakht and Diamond, 2021). An array of three infrared lights were mounted to the chamber door to track the trial period (baseline, cue, and postcue). Each grid floor bar was electrically connected to an aversive shock generator (Med Associates). An external food cup, a central port equipped with infrared photocells, and a key light were present on one wall. Auditory stimuli were generated with a WAV trigger-based device and presented through two speakers mounted on the ceiling. Each experimental chamber was enclosed in a sound-attenuating shell.

Pellet exposure and nose poke shaping

Rats were food-restricted and specifically fed to maintain their body weight throughout behavioral testing. Each rat was given four grams of experimental pellets (Bio-Serv Dustless Precision Pellets, 45 mg, Rodent Purified Diet, #F0021) in their home cage in order to overcome neophobia for 2 d. Next, the central port was removed from the experimental chamber, and rats received a 30 min session in which one pellet was delivered every minute. The central port was returned to the experimental chamber for the remainder of behavioral testing. Each rat was then shaped to nose poke in the central port for experimental pellet delivery using a fixed ratio schedule in which one nose poke into the port yielded one pellet. Shaping sessions lasted 30 min or until ∼50 nose pokes were completed. Rats not reaching at least 10 pokes received an additional session to ensure poking was learned. Each rat then received five sessions during which nose pokes into the port were reinforced on a variable interval schedule. Session 1 used a variable interval 30 s schedule (poking into the port was reinforced every 30 s on average). All remaining sessions used a variable interval 60 s schedule. For the remainder of behavioral testing, nose pokes were reinforced on a variable interval 60 s schedule independent of cue and shock presentation.

Experiment 1: pre-exposure, discrimination, and extinction testing

Each rat was pre-exposed to the two auditory cues to be used during discrimination. Auditory cues were 10 s in duration and consisted of repeating, 500 ms motifs of broadband click or trumpet. A 49 min session consisted of 10 presentations of each cue (20 total presentations) with a mean intertrial interval (ITI) of 2 min. Cue presentation order was randomly determined by the behavioral program and differed for each rat, each session.

Each rat received 10, 49 min discrimination sessions consisting of 20 trials, with a mean ITI of 2 min. Each rat received 10 threat cue and 10 neutral cue presentations. There were two probability conditions with the threat cue being followed by footshock on 10% ($n = 20$) or 30% ($n = 20$) of trials. Auditory identities of the threat and neutral cues were counterbalanced across rats. Footshock (0.5 s, 0.5 mA) was administered 2 s following cue termination on trials in which it was given. The order of threat and neutral cue presentation was randomly determined by the behavioral program and differed for each rat, each session.

Extinction testing consisted of 1, 49 min session consisting of 20 trials, with a mean ITI of 2 min. Each rat received 10 threat and 10 neutral cue presentations. No footshock was delivered during the extinction session.

Experiment 2: pre-exposure, conditioning, unconditioned stimulus inflation, and extinction testing

Each rat was pre-exposed to the 10-s tone and 10-s light cues to be used during conditioning. The tone consisted of a repeating, 500 ms broadband click motif. The light consisted of steady illumination of a cue light above the nose poke. A 64 min session consisted of three presentations of each cue (six total presentations) with a mean ITI of ∼5 min. The order of tone and light cue presentations was randomly determined by the behavioral program and differed for each rat, each session.

Each rat received two, 64 min conditioning sessions consisting of six total trials, with a mean ITI of ∼5 min. Each rat received three light-shock and three tone-shock pairings per session. Footshock (0.5 s, 0.35 mA) was administered immediately following cue termination. The order of tone-shock and light-shock trials was randomly determined by the behavioral program and differed for each rat, each session.

During unconditioned stimulus inflation, rats in the mild group received five pairings of the 10 s light with 0.5 s, 0.35 mA footshock. Rats in the intense group received five pairings of the 10 s light with 0.5 s, 3 mA footshock. Trials were evenly spaced in a condensed, 5 min session.

After a 5 min break in which the sound-attenuating chamber doors were open, rats received a tone extinction test consisting of 10, 10 s tone presentations in a single session with a mean ITI of 4 min. One week later, rats received an additional tone extinction test, followed by a light extinction test, 5 presentations in condensed 5 min session.

Calculating suppression ratio

Time stamps for auditory and visual cue presentation, shock presentation, and nose pokes (photobeam break) were automatically recorded by the Med Associates, Med-PC IV software. The baseline nose poke rate was calculated for each trial by counting the number of pokes during the 20 s precue period and multiplying by 3. The cue nose poke rate was calculated for each trial by counting the number of pokes during the 10 s cue period and multiplying by 6. Nose poke suppression was calculated as a ratio: (baseline poke rate − cue poke rate)/(baseline poke rate + cue poke rate). A suppression ratio of "1" indicated complete suppression of nose poking during cue presentation relative to baseline. A suppression ratio of "0" indicated equivalent nose poke rates during baseline and cue presentation. Gradations in suppression ratio between 1 and 0 indicated intermediate levels of nose poke suppression during cue presentation relative to baseline. Negative suppression ratios indicated increased nose poke rates during cue presentation relative to baseline.

Frame capture system

Experiment 1. Behavior frames were captured using Imaging Source monochrome cameras (DMK 37BUX28; USB 3.1, 1/2.9" Sony Pregius IMX287, global shutter, resolution 720 × 540, trigger in, digital out, C/CS-mount). Frame capture was triggered by the Med Associates behavior program. The 28 V Med Associates pulse was converted to a 5 V TTL pulse via Adapter (SG-231, Med Associates). The TTL adapter was wired to the camera's trigger input. Captured frames were saved to a PC (OptiPlex 7470 All-in-One) running the IC Capture software (Imaging Source). Frame capture began precisely 5 s before cue onset, continued throughout 10 s cue presentation, and ended 2.5 s following cue offset. This meant frames were captured during the 0.5 s shock and the 2 s following.

Experiment 2. Behavior frames were captured using Arducam day-and-night vision cameras; recordings were trial-length 1080p 30fps videos. Video capture was triggered by the Med Associates behavior program. The 28 V Med Associates pulse was converted to a 5 V TTL pulse via Adapter, with the resulting signal being read by an Arduino Uno, and interpreted by a custom Python program which in turn triggered recording in OBS Studio. Captured videos were saved to one of two Dell computers. Video capture began precisely 5 s before cue onset, continued throughout 10 s cue presentation, and ended 2.5 s following cue offset. This meant frames were captured during the 0.5 s shock and the 2 s following. Videos were then broken down into 100 frames each using every fifth frame, emulating the 5 fps framerate of the frame capture system in Experiment 1 to make hand scoring comparable across experiments.

Frame acquisition, processing, and scoring

Frames were acquired at a rate of 5 per second, with a target of capturing 100 frames per trial and 2000 frames per session. For Experiment 1, the first four threat and four neutral trials from the extinction test session were selected for scoring. A MATLAB script sorted the 32,000 frames from the eight trials into eight folders, one for each trial for reach rat, each containing 100 frames. Each 100-frame trial was made into a 100-slide PowerPoint presentation to be used for hand scoring. For Experiment 2, the first five auditory cue trials from the second extinction test session were selected for scoring. A MATLAB script sorted the 20,000 frames from the five trials into five folders, one for each trial for each rat, each containing 100 frames. Each 100-frame trial was made into a 100-slide PowerPoint presentation to be used for hand scoring.

We anonymized trial information in order to score behavior without bias. Each trial was encrypted as a unique number and/or word sequence. The trials were randomly assigned to five blind observers (Experiment 1) and four blind observers (Experiment 2). The result of trial anonymization was that observers were completely blind to the subject, group, and trial. Furthermore, random assignments ensured that the trials from a single rat were scored by different observers.

Frames were scored using a specific procedure. Frames were first watched in real time in Microsoft PowerPoint by setting the slide duration and transition to 0.19 s and then playing as a slideshow. Behaviors

clearly observed were noted. Next, the observer went through all the frames scoring one behavior at a time. A standard scoring sequence was used: port, cup, rear, scale, jump/hang, groom, freeze, locomote, backpedal, and stretch. When the specific behavior was observed in a frame, that frame was labeled. Once all behaviors had been scored, the video was rewatched for freezing. In our procedure, cup is defined based on the rat's location, and freezing is defined based on the rat's behavior. If the two co-occurred, the cup superseded freezing because it was prevalent during the baseline behavior. The unlabeled frames were then labeled "background." Finally, all background frames were checked to ensure they did not contain a defined behavior.

Definitions

Background. Specific behavior cannot be discerned, often because rat is turned away from camera or position of forepaws is not clear or rat is not engaged in any other behavior.

Cup. Any part of the nose above the food cup but below the nose port.

Freeze. Arched back, stiff rigid posture in the absence of movement, all four limbs on the floor (often accompanied by hyperventilation and piloerection). Side-to-side head movements and up-and-down head movements that do not disturb rigid posture are permitted. Activity such as sniffing or investigation of the bars is not freezing. Freezing, as opposed to pausing, is likely to be 3+ frames (600+ ms) long.

Groom. Any scratching, licking, or washing of the body.

Jump/hang. All four limbs off the floor and back two feet off of wall. This includes hanging which is distinguished when hind legs are hanging freely.

Backpedal. Rapid backward displacement of the body. Often (not always) the head is down, and/or the back is arched. Backward component of movement must be stronger than the lateral component. A lateral movement is not a backpedal. Backpedal considers the current frame (t) and the next two frames ($t+1$ and $t+2$). By frame $t+2$ the body and both back feet must be displaced backward relative to frame t. The rat can move the body and both feet by $t+1$ and $t+2$ or move in combination of both frames; all count as backpedal for trial t.

Locomote. Propelling body across chamber on all four feet, as defined by movement of back feet. Movement of the back feet with the front feet off the floor is rearing. Locomote considers the current frame (t) and the next two frames ($t+1$ and $t+2$). By frame $t+2$, the body and both back feet must be displaced forward relative to frame t. The rat can move the body and both feet by $t+1$ and $t+2$ or move in combination of both frames; all count as locomote for trial t.

Poke. Any part of the nose in the port or the nose is obscuring the infrared indicator inside the port. Often standing still in front of the port but sometimes tilting the head sideways with the body off to the side of the port.

Rear. At least one hind leg is on the grid floor with both forepaws off the grid floor. Often (not always) stretching to full extent, forepaws usually (not always) on top of the side walls of chamber, often pawing the walls; may be accompanied by sniffing or slow side-to-side movement of the head. Does not include grooming movements or eating, even if performed while standing on hind legs.

Scale. All four limbs are off the floor, but at least one limb is on the side of the chamber. Standing on the food cup counts as scaling.

Stretch. Body elongated with belly touching or nearly touching the grid bars. Body posture often appears flatter than that rat's natural posture.

Histology

Upon the conclusion of behavioral testing, rats were anesthetized with an overdose of isoflurane and perfused intracardially with 0.9% biological saline and then 10% neutral-buffered formalin. Brains were extracted and postfixed in 10% neutral-buffered formalin for 24 h and then stored in 4% formalin and 10% sucrose for an additional 24 h. Forty micrometer sections were collected on a sliding microtome and stored in cryoprotectant until mounting.

To represent the totality of the PAG, we determined starting with a slice at −6.00 mm from bregma and then decreasing by 0.5 until −8.50 mm (six samples) would span the desired area of the PAG. Free-floating brain sections were processed for NeuroTrace fluorescent Nissl staining. Sections were rinsed in 0.05 M KPBS (three times for 5 min) and incubated for 1 h at room temperature in the dark with NeuroTrace 435/455 Blue (Thermo Fisher Scientific, #*N*21479) diluted 1:200 in KPBS containing 0.1% Triton X-100. After incubation, the tissue was washed in KPBS (three times for 5 min), mounted on unsubbed slides, air-dried, and coverslipped with Vectashield Hardset mounting medium (Vector, #H-1400, without DAPI). Slides were stored at −20°C and imaged within 3 weeks to prevent fluorescence degradation.

Image acquisition, neuron quantification, and mapping

Within a week of the mounting process, slices were imaged using a light microscope (Axio Imager Z2, Zeiss). Images of the slices were individually opened with ImageJ (Fiji). Using the rat brain atlas as a reference, we cut out PAG for each individual image. A representative selection of these images was then uploaded to Ilastik for training, totaling 24 images. These images were selected to represent each condition: male, female, control infusion, and AAV infusion. These images were also selected based on their variations in brightness and clarity in order to encompass a variety of image appearances. From these images, we went through and labeled "cell" and "background" by drawing lines and dots through neurons to train the program to identify cells versus areas we wanted to designate background. We did this for ∼20–30 cells for each image, picking out a variety of cell shapes, brightness, and clarity. After training, the threshold was set at 0.15, and the pixel size was set to 4 for specificity. This allowed the maximum amount of neurons to be counted without including background. The information was processed as simple segmentations, which exported a binary mask of the PAG cutout image as a tiff, as well as a CSV file that detailed neuron counts for each image and details about each neuron counted. The remaining images were then batch processed so all 240 images were processed and had a respective mask and CSV file of their neuron counts.

These images were also used to make mappings of deletion extent. Using rat brain atlas image overlays and Adobe Illustrator, each of the six brain levels was outlined. For all of the deletion rats at all six levels, the images were used to create a semi-opaque shape depicting the extent of neuronal death both within and beyond the PAG. All the deletion shapes were overlayed to create a depiction of the totality of neuronal deletion caused by the procedure.

Statistical analyses

Neuron number, baseline nose poke rate, and suppression ratio data were analyzed with analysis of variance (ANOVA); $p < 0.05$ was considered significant. Within-subject, post hoc comparisons were performed using dependent-sample t tests. Between-subject, post hoc comparisons were performed using independent-sample t tests; $p < 0.05$ was considered significant. Correlation coefficients were computed using Pearson's r. Ethogram data were analyzed with multivariate analysis of variance (MANOVA) for the 10 ethogram behaviors follow by ANOVA. Hotelling's T^2 test was used to examine whether multivariate patterns differed between groups; $p < 0.05$ was considered significant.

We applied linear discriminant analysis (LDA) to determine whether multivariate profiles measured during the threat cue could predict group membership across four conditions: Control 10%, Control 30%, PAGd 10%, and PAGd 30%. For each subject, we constructed feature vectors from the ethogram recorded during the threat cue and trained LDA classifiers (MATLAB fitcdiscr, pseudo-linear). To assess robustness and chance performance, the full pipeline was run for 200 iterations.

In each iteration, we (1) trained an LDA model using the true group labels and a matched null model with shuffled labels; (2) performed k-fold cross-validation (10-fold) and recorded k-fold loss and cross-validated predictions; and (3) computed 4×4 confusion matrices (actual × predicted) and column-normalized percentages for interpretability. We summarized classification accuracy per iteration and compared true-label models against shuffled-label baselines using independent-sample t tests ($\alpha = 0.05$). For cell-wise evaluation of confusion matrices, we contrasted corresponding cells between true and shuffled models with Bonferroni's correction across the 16 matrix cells. To test whether classification was driven by a single group, we repeated the entire pipeline excluding the Control 30% group and re-evaluated cross-validated loss, accuracy, and confusion-matrix contrasts.

Results

Experiment 1

Forty Long–Evans rats received viral infusions targeting the ventrolateral PAG (Fig. 1*A*). Control rats ($n = 21$, 10 females) received four 0.5 µl infusions of a 40/60 mixture AAV2-eSyn-EGFP-T2A-iCre-WPRE and 0.9% biological saline. Two infusion sites bilaterally targeted the anterior ventrolateral PAG: AP −7.10, ML ±1.42, DV −5.89. The remaining two infusion sites targeted the posterior ventrolateral PAG: AP −8.00, ML ±1.60, DV −6.04. Both infusions were performed at a 10° angle. PAGd rats ($n = 19$, 10 females) received four 0.5 µl infusions of a 50/50 mixture of AAV2-eSyn-EGFP-T2A-iCre-WPRE + AAV-flex-taCasp3-TEVp. The deletion coordinate approach was identical to the control approach above. AAV2-eSyn-EGFP-T2A-iCre-WPRE tags neurons with cre, while AAV-flex-taCasp3-TEVp selectively induces apoptosis in cre-tagged neurons (Yang et al., 2013). This surgical/AAV approach was chosen to ensure robust neuronal deletion along the anterior–posterior span of the ventrolateral and lateral PAG subregions in PAGd rats but not control rats.

The trade-off for achieving high deletion penetrance was lesser specificity: deletion outside of the lateral and ventrolateral subregions. This trade-off was intentional. No prior study had demonstrated a PAG role in probability-dependent scaling of fear responding or in updating threat predictions. Rigorously testing each role required an approach that would permit meaningful negative findings. Intact scaling of fear responding or intact unconditioned stimulus inflation, following high-penetrance deletion, would be strong evidence that the PAG is dispensable for these functions.

Following recovery, rats in each surgical condition were assigned to one of two discrimination groups (Fig. 1*B*). In both groups, a threat cue predicted footshock while a neutral cue did not. The threat cue was followed by shock on 30% of trials for the 30 group but on 10% of trials for the 10 group. Prior work from our laboratory has shown that both groups acquire differential fear responding (threat > neutral) that scales to shock probability (30 > 10%; Russell and McDannald, 2024). After behavioral testing, rats were perfused with saline and formalin; brains were extracted, postfixed in formalin and 10% sucrose, and then frozen, sectioned, and processed with NeuroTrace. To quantify neuron number across the anterior–posterior extent, we processed six sections per rat, spaced by ∼0.5 mm, starting at bregma −6.00 and ending at bregma −8.50. Subregion-specific and bregma-level–specific neuron counts were obtained using Ilastik, an interactive machine-learning image analysis tool that performs pixel-based classification to segment neurons from background (Berg et al., 2019). ANOVA for neuron counts was performed for each subregion (five: dPAG, dlPAG, lPAG, vlPAG, and vmPAG) with the following factors: AAV (Control vs PAGd); bregma level (−6.00, −6.50, −7.00, −7.50, −8.00, and −8.50); sex (female vs male); and group (30 vs 10). The "vmPAG" is composed of different brain regions along the anterior–posterior axis. We discuss the nature of this deletion after the results.

The primary ANOVA results are shown in Table 1. Relative to control rats, PAGd rats showed significant reductions in neuron number in all subregions except for the dorsal PAG (data in Fig. 1*C*; visualizations in Fig. 1*D*). Deletion was most pronounced between bregma levels −7.00 and −8.00 in the lateral, ventrolateral, and ventromedial subregions. Representative Control and PAGd histology is shown in Supplemental Figure 1. Complete mappings of deletion extent are shown in Figure 2*A*. With histology confirming robust neuronal deletion, final group numbers were as follows: Control 30 ($n = 9$; four females), Control 10 ($n = 12$; six females), PAGd 30 ($n = 11$; six females), and PAGd 10 ($n = 8$; four females).

PAG neuronal deletion increases baseline nose poking during conditioning

Rats were shaped to nose poke for food pellets, and nose poking was reinforced on a variable interval 60 s schedule during each session. On average, baseline nose poke rates increased across the 11 sessions (pre-exposure→Session 10). Control patterns differed as a function of shock probability (Fig. 3*A*,*B*). Control 30 rats decreased baseline poking following shock introduction, then increased after Session 3. Control 10 rats showed no such decreases. PAGd rat baseline nose poke rates were insensitive to probability. Neither PAGd 30 nor PAGd 10 rats decreased poking following footshock introduction, and PAGd rats showed higher overall baseline nose poke rates. In support of these descriptions, ANOVA for baseline nose poke rate with factors session (11, pre-exposure→session 10), sex (female vs male), AAV (Control vs PAGd), and group (30 vs 10) revealed significant main effects of session ($F_{(10,320)} = 19.98$, $p = 2.56 \times 10^{-27}$) and AAV ($F_{(1,32)} = 10.52$, $p = 0.003$). ANOVA further revealed significant interactions for session × AAV ($F_{(10,320)} = 2.29$, $p = 0.013$), session × group ($F_{(10,320)} = 5.95$, $p = 2.89 \times 10^{-8}$), and session × AAV × group ($F_{(10,320)} = 2.13$, $p = 0.022$). Males increased poking more greatly over the final five sessions, finishing with higher rates (sex × session, $F_{(10,320)} = 2.16$, $p = 0.02$). No other sex interactions were found.

PAG neuronal deletion reduces cue-elicited nose poke suppression during conditioning

Cue-elicited nose poke suppression (measured via suppression ratio) was used as a general index of behavioral responding to the threat and neutral cues (Estes and Skinner, 1941). All rats initially showed equivalent nose poke suppression levels to the threat and neutral cues. Differential responding emerged around Session 5 and was maximal by Session 10. Control 30 rats (Fig. 3*C*) demonstrated higher levels of suppression than Control 10 rats (Fig. 3*D*). PAGd 30 rats (Fig. 3*E*) also demonstrated higher levels of nose poke suppression than PAGd 10 rats (Fig. 3*F*). However, PAGd rats showed slower overall acquisition of nose poke suppression and exhibited lower overall suppression. This reduction meant that Control 10 and PAGd 30 rats showed similar nose poke suppression patterns across sessions. PAGd 10 rats showed the lowest overall responding. ANOVA for suppression ratio with factors session (11, pre-exposure→session 10), sex (female vs male), AAV:(Control vs PAGd), cue (threat vs neutral), and group (30 vs 10) revealed

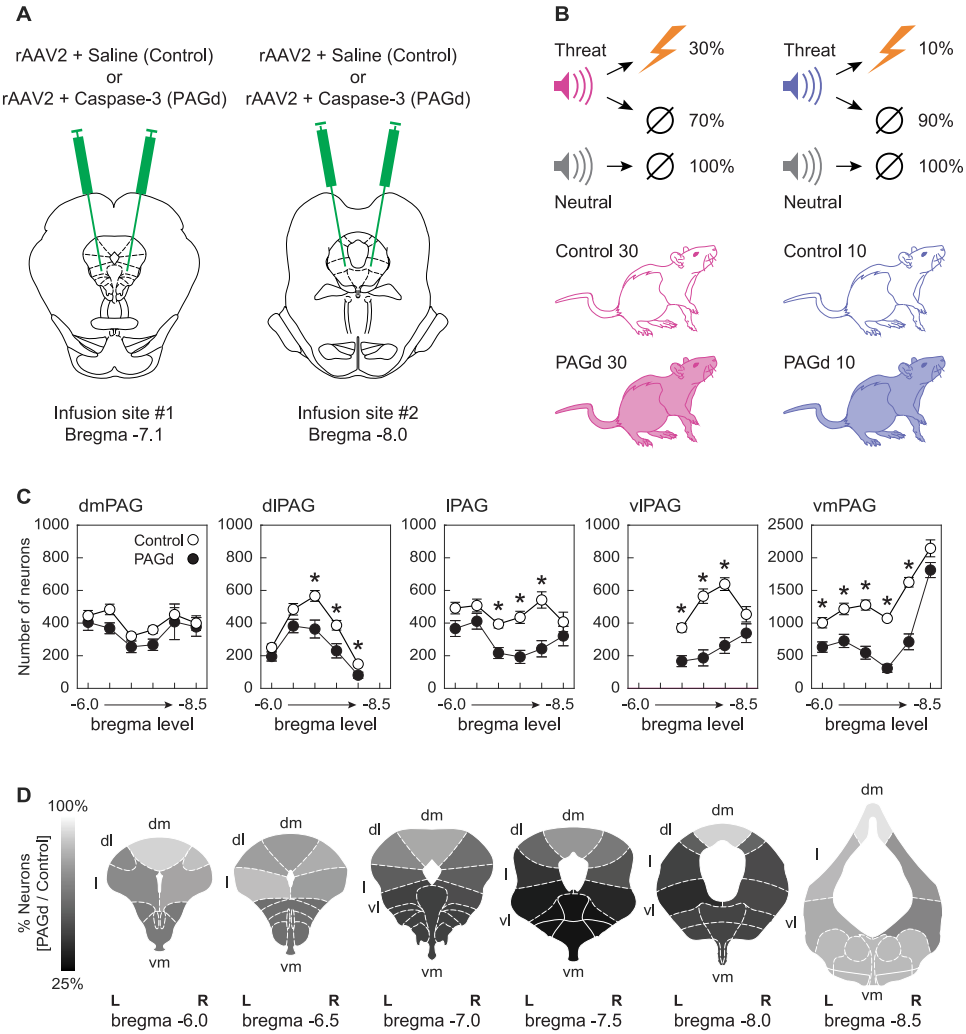


Figure 1. Experiment 1 design and histology. ***A***, Control rats received bilateral infusions of rAAV2 + saline while PAGd rats received bilateral infusions of rAAV2 + cre-dependent caspase-3 in the anterior (−7.10) and posterior (−8.00) PAG. ***B***, Following recovery, rats received fear discrimination in which a threat auditory predicted shock with 30% (magenta, top left) or 10% (blue, top right) footshock. A neutral cue (gray) never predicted footshock. The total experimental design yielded four groups: Control 30, Control 10, PAGd 30, and PAGd 10 (***B***, bottom). ***C***, Mean ± SEM neuron number for Control (open symbols) and PAGd (closed symbols) rats is shown for five periaqueductal subregions (dmPAG, dorsomedial; dlPAG, dorsolateral; lPAG, lateral; vlPAG, ventrolateral; and vmPAG, ventromedial), across six bregma levels (−6.0, −6.5, −7.0, −7.5, −8.0, and −8.5). ***D***, The percentage of deletion is visualized as the percentage of neurons per region/bregma level in PAGd rats compared with controls. Gradient extremes are black (25% of control neuron levels) to white (100% of control neuron levels). *Significance of an independent samples, Bonferroni-corrected *t* test.

Table 1. ANOVA results for neuron number quantification, Experiment 1

PAG subregion	AAV main effect		Bregma main effect		AAV × bregma interaction	
Dorsal	$F_{(1,32)} = 1.64$	$p = 0.21$	$\mathbf{F_{1,32} = 5.98}$	$\mathbf{p = 4.25 \times 10^{-5}}$	$F_{(5,160)} = 0.55$	$p = 0.73$
Dorsolateral	$\mathbf{F_{(1,32)} = 15.80}$	$\mathbf{p = 3.75 \times 10^{-5}}$	$\mathbf{F_{(1,32)} = 100.59}$	$\mathbf{p = 1.53 \times 10^{-38}}$	$\mathbf{F_{(5,160)} = 4.84}$	$\mathbf{p = 0.001}$
Lateral	$\mathbf{F_{(1,32)} = 20.58}$	$\mathbf{p = 7.61 \times 10^{-5}}$	$\mathbf{F_{(1,32)} = 9.94}$	$\mathbf{p = 2.71 \times 10^{-8}}$	$\mathbf{F_{(5,160)} = 5.00}$	$\mathbf{p = 2.78 \times 10^{-5}}$
Ventrolateral	$\mathbf{F_{(1,32)} = 48.15}$	$\mathbf{p = 7.39 \times 10^{-8}}$	$\mathbf{F_{(1,32)} = 16.67}$	$\mathbf{p = 1.27 \times 10^{-9}}$	$\mathbf{F_{(5,160)} = 15.53}$	$\mathbf{p = 2.61 \times 10^{-8}}$
Ventral*	$\mathbf{F_{(1,32)} = 45.80}$	$\mathbf{p = 1.20 \times 10^{-7}}$	$\mathbf{F_{(1,32)} = 86.910}$	$\mathbf{p = 8.60 \times 10^{-44}}$	$\mathbf{F_{(5,160)} = 5.78}$	$\mathbf{p = 6.23 \times 10^{-5}}$

F and *p* values are shown for the main effects of AAV (Control vs PAGd) and bregma level and their interaction on neuron number within each PAG subregion (dorsal, dorsolateral, lateral, ventrolateral, ventromedial). Bold indicates ANOVA significance.

significant main effects of cue ($F_{(1,31)} = 18.71$, $p = 6.46 \times 10^{-12}$), session ($F_{(10,310)} = 1.89$, $p = 1.14 \times 10^{-43}$), AAV ($F_{(1,31)} = 15.12$, $p = 0.0005$), and group ($F_{(1,31)} = 14.04$, $p = 0.001$). ANOVA further revealed significant interactions for session × AAV ($F_{(10,320)} = 4.15$, $p = 0.001$), session × group ($F_{(10,320)} = 6.64$, $p = 2.46 \times 10^{-9}$), and cue × session ($F_{(10,320)} = 30.15$, $p = 2.86 \times 10^{-40}$). No significant main effect of sex or interaction with sex was found.

PAG neuronal deletion decreases cue-elicited nose poke suppression and increases baseline nose poking during extinction

Nose poke suppression patterns observed during discrimination persisted in extinction (Fig. 4*A–D*). All rats showed greater nose poke suppression to the threat cue that, on average, decreased over trials. PAGd rats showed lower overall suppression levels

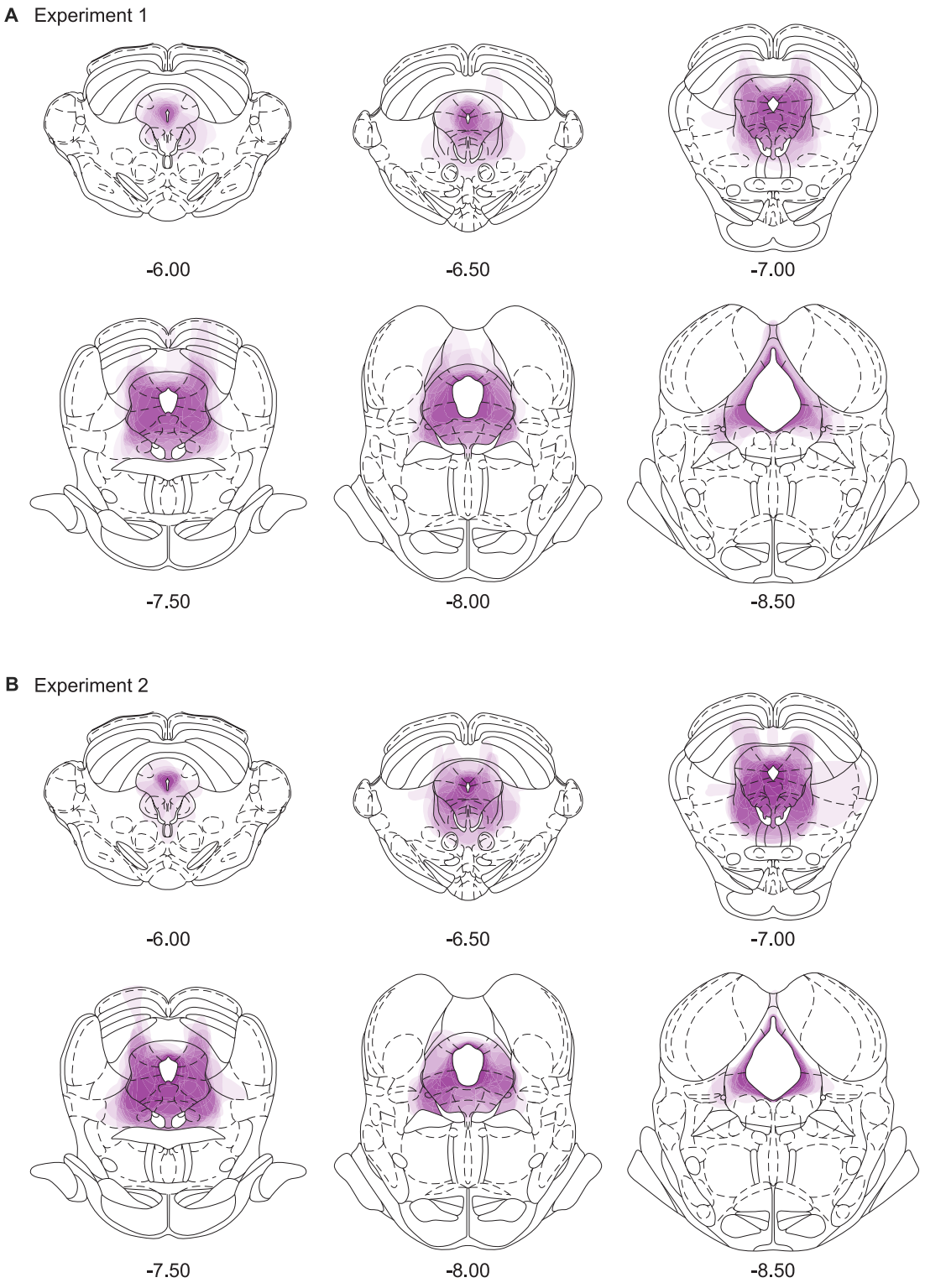


Figure 2. Maps of brainstem deletion extent. ***A***, Deletion extent is shown for PAGd rats in Experiment 1 across six coronal sections spanning bregma −6.00 to −8.50 in 0.5 mm increments. ***B***, Deletion extent is shown for PAGd rats in Experiment 2 across the same six coronal sections. For both panels, the deletion extent of each PAGd rat was individually traced, rendered transparent, and overlaid. Darker purple regions indicate areas of more consistent neuronal deletion across rats.

compared with Control rats. During extinction, PAGd rats poked at higher baseline nose poke rates than Control rats (Fig. 4*E*). ANOVA for suppression ratio with factors trial (10 per cue), sex (female vs male), AAV (Control vs PAGd), cue (threat vs neutral), and group (30 vs 10) revealed significant main effects of cue ($F_{(1,32)} = 69.33$, $p = 1.63 \times 10^{-9}$), trial ($F_{(9,288)} = 4.34$, $p = 2.52 \times 10^{-5}$), and AAV ($F_{(1,32)} = 6.63$, $p = 0.015$). ANOVA further revealed a significant interaction for cue × trial ($F_{(9,288)} = 2.51$, $p = 0.009$). Significant baseline nose poke differences were confirmed with an independent-sample t test comparing mean baseline nose poke rate for all Controls vs all PAGd ($t_{(38)} = 2.33$, $p = 0.025$). Although PAGd rats showed decreased nose poke suppression and elevated

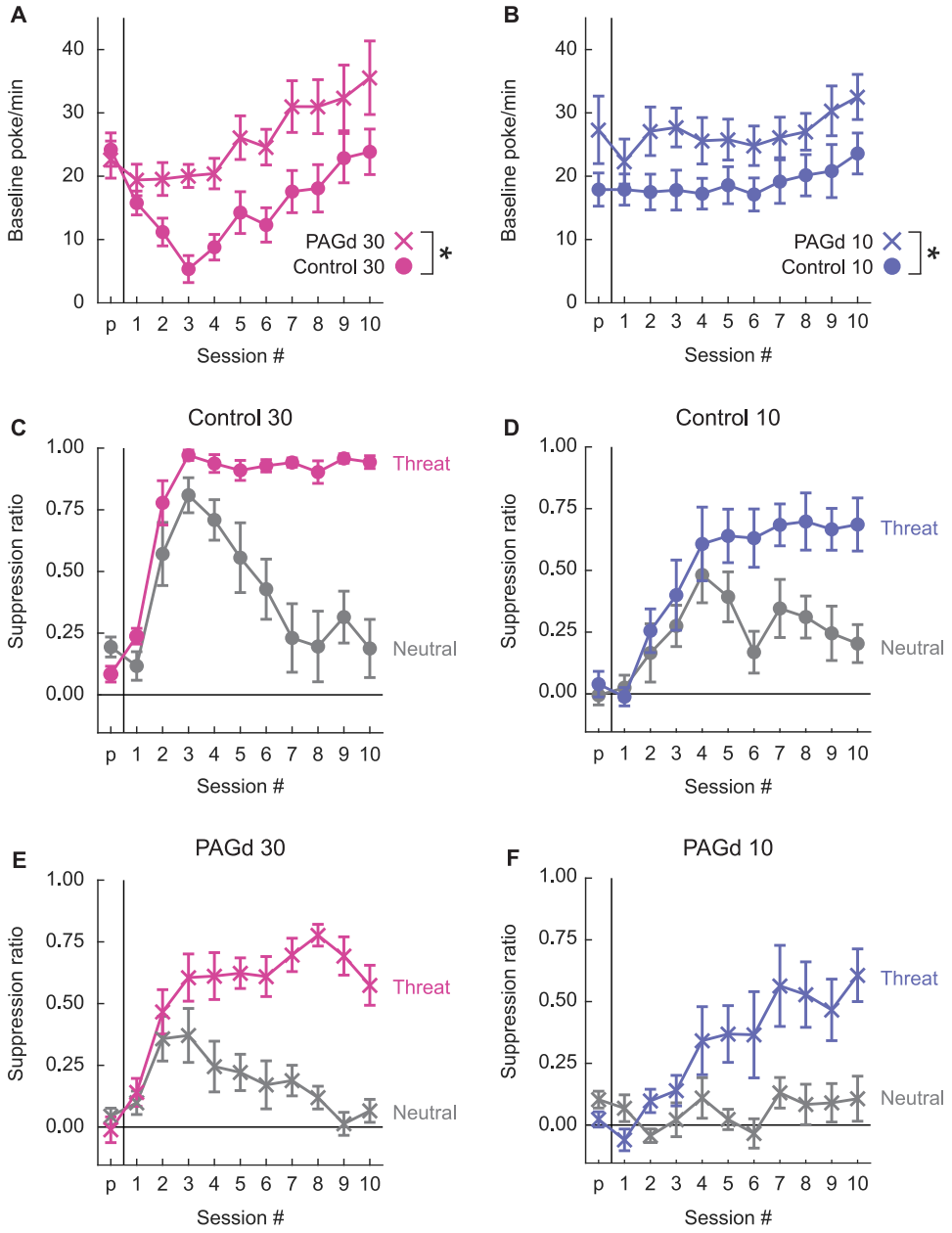


Figure 3. Responding during conditioning. ***A***, Mean ± SEM baseline nose poke rate (poke/min) is shown for Control 30 (magenta, circles) and PAGd 30 (magenta, Xs) rats for pre-exposure and the 10 conditioning sessions. ***B***, Mean ± SEM baseline nose poke rate (poke/minute) is shown for Control 10 (blue, circles) and PAGd 10 (blue, Xs) rats. ***C***, Mean ± SEM suppression ratio is shown for Control 30 rats for the threat cue (magenta) and neutral cue (gray). ***D***, Mean ± SEM suppression ratio is shown for Control 10 rats for the threat cue (blue) and neutral cue (gray). ***E***, Mean ± SEM suppression ratio is shown for PAGd 30 rats for the threat cue (magenta) and neutral cue (gray). ***F***, Mean ± SEM suppression ratio is shown for PAGd 10 rats for the threat cue (blue) and neutral cue (gray).

baseline nose poking, these effects were unrelated. Comparing mean baseline nose poke rate to mean cue suppression ratio found zero correlation for the threat cue (Fig. 4*F*; $r = -0.004$, $p = 0.98$) and the neutral cue (Fig. 4*G*; $r = -0.12$, $p = 0.45$).

Subsecond ethograms spanning 10 behaviors

So far, our results reveal dual roles for the PAG to determine learning rate (Johansen et al., 2010) and asymptotic responding (McNally et al., 2011) when measuring responding with nose poke suppression (Amorapanth et al., 1999). Still, conditioned suppression can be achieved through many behavioral and neural mechanisms. Revealing specific roles for the PAG in probability-dependent scaling of fear responding requires a more detailed approach.

To do this, we constructed comprehensive, high-temporal-resolution ethograms during extinction testing. Frames were sampled every 200 ms, beginning 5 s before cue onset, ending 5 s after cue offset, and scored for 10 behaviors: groom, poke, cup, backpedal, locomote, jump, scale, rear, stretch, and freeze (see Materials and Methods). Frames were scored by five observers blind to trial type and group. To assess inter-rater reliability, each of the five observers scored an identical set of comparison trials. Mean identical observations for the comparison trials across the five scorers was 80.46%, indicating robust scoring consistency. Ethograms were constructed for the first four threat and neutral trials. These trials were selected based on ANOVA finding no main effect of AAV on suppression ratio ($F_{(1,32)} = 1.49$, $p = 0.23$). This result confirmed no gross differences in cue-

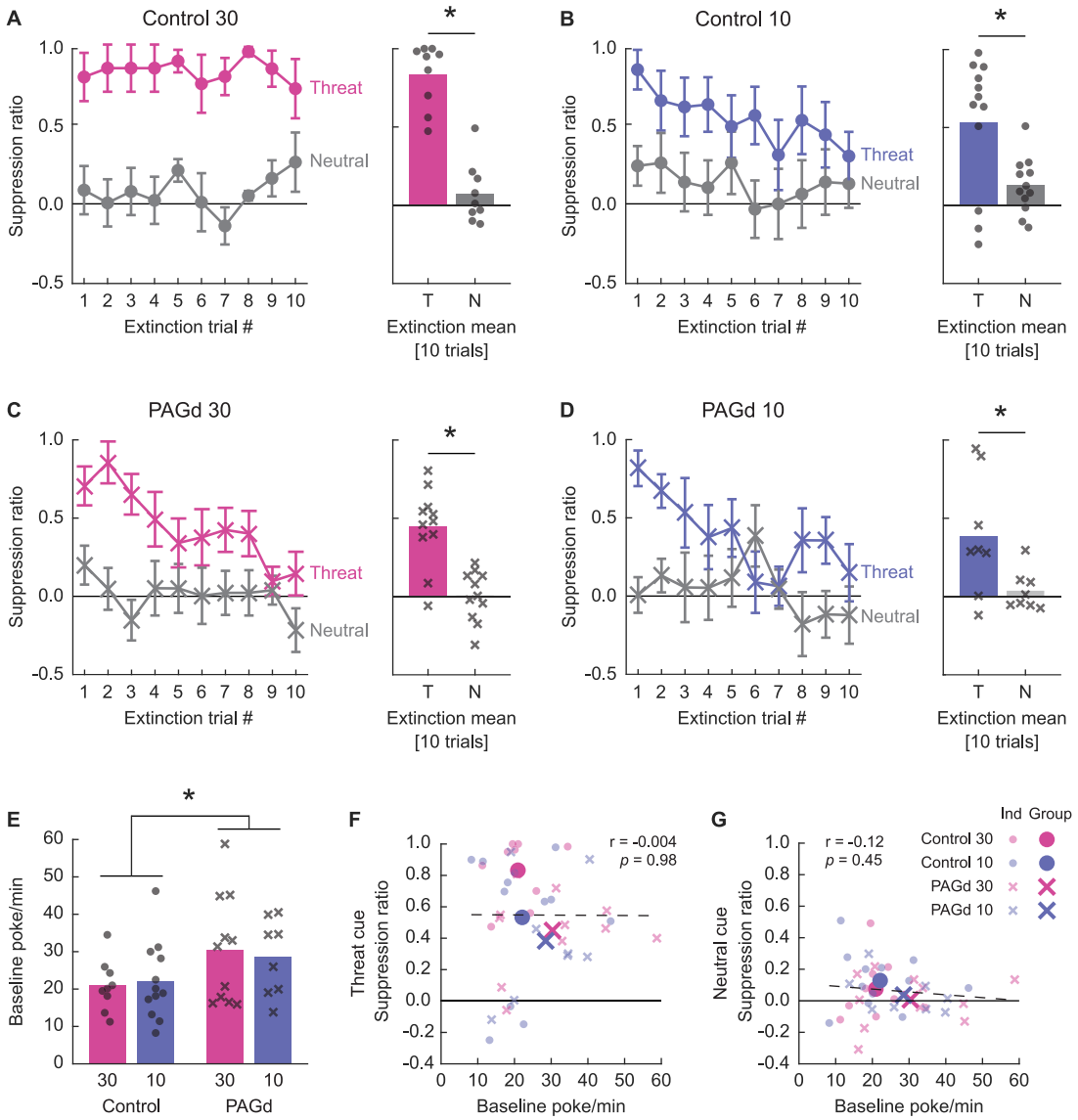


Figure 4. Responding during extinction. ***A***, Left, Mean ± SEM suppression ratio is shown for Control 30 rats for the threat cue (magenta) and neutral cue (gray) for the each of the 10 extinction trials. ***A***, Right, Group (bar) and individual (circles or Xs) mean suppression ratio for all 10 trials is shown for the threat cue (T) and neutral cue (N). Identical plots are shown for (***B***) Control 10 rats, (***C***) PAGd 30 rats, and (***D***) PAGd 10 rats. *(***A–D***) significance of a dependent-sample *t* test ($p < 0.05$). ***E***, Group (bar) and individual (circles and Xs) mean baseline nose poke rate for all 10 trials is shown for all groups. *significance of an independent-sample *t* test ($p < 0.05$). ***F***, Scatterplot compares group (large, opaque symbols) and individual (small, transparent symbols) baseline nose poke rate (*x*-axis) versus threat suppression ratio (*y*-axis). The dotted line indicates linear trend across all rats. ***G***, The same relationship is plotted for the neutral cue.

driven behavior between Control and PAGd rats, allowing for specific responding differences to emerge.

Complete ethograms are shown for Control 30 rats (Fig. 5*A*), Control 10 rats (Fig. 5*B*), PAGd 30 rats (Fig. 5*C*), and PAGd 10 rats (Fig. 5*D*). Overall, Control rats showed differential responding to threat and neutral cues that was sensitive to time and probability (30 > 10% during early cue presentation). PAGd rats showed differential responding to threat and neutral cues, but fear responding was insensitive to probability. Specifically, PAGd 30 rats showed fear responding that was comparable to PAGd 10 and Control 10 rats.

PAG neuronal deletion increases baseline rearing and locomotion

We chunked the 20 s ethogram data into four 5 s periods: baseline, early cue, late cue, and post cue. We first performed MANOVA for all 10 behavior categories with factors time (25, 200 ms intervals), sex (female vs male), AAV (Control vs PAGd), group (30 vs 10), and cue (threat vs neutral) for the 5 s baseline period. MANOVA revealed only a significant main effect of AAV ($F_{(9,34)} = 2.63$, $p = 0.028$). Univariate ANOVA revealed this main effect to be driven primarily by differences in locomotion (PAGd > Control; $F_{(1,32)} = 15.78$, $p = 3.78 \times 10^{-4}$) and rearing (PAGd > Control; $F_{(1,32)} = 9.11$, $p = 0.005$). PAGd rats showed higher baseline locomotion and rearing than Control rats (Fig. 5*D*). The mean percentage of baseline rearing and locomotion was positively correlated across individuals (Fig. 5*E*; $r = 0.39$, $p = 0.012$). The combined baseline rearing/locomotion profile differed between Control and PAGd rats. Hotelling's T^2 test for the joint distribution of baseline rearing and locomotion confirmed significant multivariate separation between Control and PAGd rats ($T^2 = 18.15$, equivalent $F_{(2,37)} = 8.84$, $p = 7.29 \times 10^{-4}$).

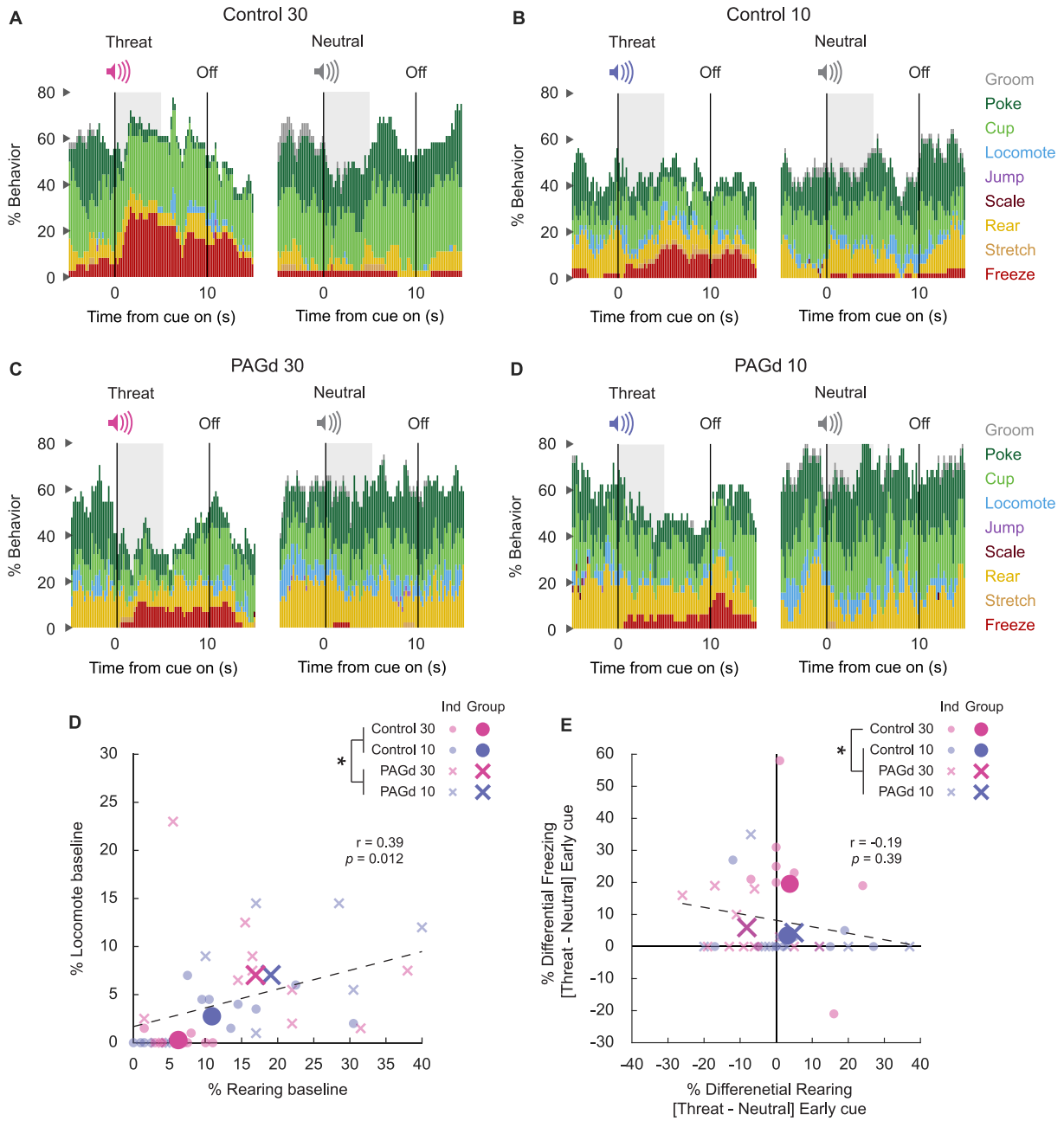


Figure 5. Ethograms. ***A***, The mean percentage of behavior (*y*-axis) before, during, and after the cue period (*x*-axis) for the threat (magenta, left) and neutral (gray, right) cues for the control 30 rats. The behaviors included (gray) groom, (dark green) poke, (light green) cup, (light blue) locomotion, (purple) jump, (maroon) scale, (yellow) rear, (orange) stretch, and (red) freeze. Light gray rectangle indicates the early cue period (first 5 s). Identical plots are shown for (***B***) Control 10 rats, (***C***) PAGd 30 rats, and (***D***) PAGd 10 rats. ***E***, Scatterplot compares group (large, opaque symbols) and individual (small, transparent symbols) percentage of locomotion baseline (*y*-axis) versus the percentage of rearing baseline (*x*-axis). The dotted line indicates linear trend across all rats. ***F***, Scatterplot compares group (large, opaque symbols) and individual (small, transparent symbols) percentage of freezing first half threat − neutral (*y*-axis) versus the percentage of rearing first half threat − neutral (*x*-axis). The dotted line indicates the linear trend across all rats. *Significance of an independent-sample *t* test ($p < 0.05$).

PAG neuronal deletion eliminates early cue probability-dependent behavior scaling

Next, we performed MANOVA (dependent variables and factors as above) for the early cue period. Now MANOVA revealed a significant main effect of cue ($F_{(8,25)} = 6.11$, $p = 0.0002$) and a significant AAV × group × cue interaction ($F_{(8,25)} = 2.78$, $p = 0.024$). Univariate ANOVA revealed the main effect of cue to be driven by freezing (threat > neutral; $F_{(1,32)} = 3.68$, $p = 0.0002$) and poking (neutral > threat; $F_{(1,32)} = 6.16$, $p = 1.26 \times 10^{-5}$). Univariate ANOVA revealed the AAV × group × cue interaction to be driven by multiple behaviors. Control 30 rats showed unique, differential responding (threat vs neutral) that was distinguishable from all other groups. Control 10, PAGd 30, and PAGd 10 rats showed comparable behavioral patterns.

In support, univariate ANOVA found trends toward AAV × group × cue interaction significance for freezing ($F_{(1,32)} = 2.94$, $p = 0.096$), rearing ($F_{(1,32)} = 3.07$, $p = 0.089$), and stretching ($F_{(1,32)} = 3.17$, $p = 0.085$), but not outright individual significance. Instead, probability-dependent scaling of responding was captured by multiple behaviors and neuronal deletion disrupted this multi-behavior pattern. To demonstrate, we plotted the mean percentage of differential freezing (threat − neutral) against

the mean percentage of differential rearing (Fig. 5*E*). There was no significant relationship between the two measures ($r = -0.19$, $p = 0.39$). However, the individual and group distributions revealed the nature of the interaction. Control 30 rats showed higher differential freezing than all other rats, which were equivalent. PAGd 30 rats showed inverted differential rearing (neutral > threat) which differed from all other rats. The combined freezing/rearing profile highlighted the Control 30 rats as unique. Hotelling's T^2 test for the joint distribution of differential freezing and differential rearing confirmed significant multivariate separation between Control 30 rats and all other rats ($T^2 = 12.71$, equivalent $F_{(2,37)} = 6.19$, $p = 0.005$). PAGd 30 rats were not unique and did not show multivariate separation from all other rats ($T^2 = 1.30$, equivalent $F_{(2,40)} = 0.64$, $p = 0.53$).

Significant AAV × group × cue interactions were restricted to the early cue period. MANOVA (dependent variables and factors as above) for the late cue period found only a significant main effect of cue ($F_{(9,24)} = 5.85$, $p = 0.0002$). Univariate ANOVA for the late cue period found significant main effects of cue for freezing (threat > neutral; $F_{(1,32)} = 14.67$, $p = 0.001$), poke (neutral > threat; $F_{(1,32)} = 42.87$, $p = 2.34 \times 10^{-7}$), and locomote (neutral > threat; $F_{(1,32)} = 6.76$, $p = 0.014$). MANOVA for the postcue period revealed only a significant main effect of cue ($F_{(9,24)} = 9.30$, $p = 5.85 \times 10^{-6}$). Univariate ANOVA for the postcue period found significant main effects of cue for freezing (threat > neutral, $F_{(1,32)} = 3.36$, $p = 2.42 \times 10^{-4}$), rearing (neutral > threat; $F_{(1,32)} = 6.96$, $p = 0.013$), and poking (neutral > threat, $F_{(1,32)} = 3.36$, $p = 5.96 \times 10^{-6}$). Equivalent late cue and postcue responding in Control and PAGd rats means that the early cue deficit cannot be attributed to general response decrements.

Baseline rearing and locomotion are unrelated to threat-elicited freezing

Ethograms reveal elevated baseline rearing and locomotion in PAGd rats, followed by reduced early cue freezing. A parsimonious account for these findings is behavioral momentum. PAGd rats enter the cue period more active than Control rats. This momentum competes more effectively with freezing, reducing the total freezing levels. If this were the case, one would expect to observe a negative relationship between baseline rearing/locomotion and early cue freezing. Trials with higher baseline rearing and locomotion would be predicted to have lower early cue freezing and vice versa. To examine this possibility, we isolated the individual threat trials for all groups/rats (Control 30–36 trials; Control 10–48 trials; PAGd 30–44 trials; and PAGd 10–32 trials; Supplemental Fig. 2). We then plotted rearing (1), locomotion (2), and freezing (3) across the total time period for each trial. Comparing mean baseline locomotion (blue) and rearing (yellow) to mean early cue freezing found zero correlation for all behavior–behavior comparisons (Control 10; PAGd 30; PAGd 10; and Control 30; all $r < |0.2|$, all $p > 0.2$). Reduced early cue freezing by PAGd rats cannot be attributed to increased baseline locomotion and rearing.

Linear classification confuses PAGd groups for each other and for Control 10 rats

MANOVA and multivariate pattern separation findings suggest that PAG neural deletion nullifies increased fear responding brought on by increased threat probability (10→30%). As a consequence, PAGd 30 rats became behaviorally indistinguishable from the low threat probability Control and PAGd rats (10%).

To directly address this, we iteratively applied LDA, which uses a reverse inference compared with MANOVA/ANOVA. LDA asks whether multivariate behavioral patterns are distinctive enough to predict the group membership of individual rats. If Control 30 rats exhibit a unique fear responding profile, LDA should classify these rats well. If PAG neuronal deletion reduces PAGd 30 fear responding to PAGd/Control 10 levels, LDA should misclassify these groups for one another. LDA was used to classify the four AAV/group combinations (Control 30, Control 10, PAGd 30, PAGd 10) based on their complete threat ethograms. To establish chance classification, we performed LDA on datasets for which group membership and ethogram were shuffled. Group classification based on ethograms (mean 36.55% accuracy across 200 models) exceeded shuffled classification (mean 26.93% across 200 models) as revealed by an independent-sample t test ($t_{(198)} = 10.51$, $p = 8.43 \times 10^{-21}$; Fig. 6*A*). Despite significance, ethogram classification accuracy was only ~10% higher than shuffled accuracy, indicating substantial misclassification.

To understand where classification errors occurred, we constructed confusion matrices (Fig. 6*B*,*C*). Each 4 × 4 matrix plots predicted group (*x*-axis) against actual group (*y*-axis), with mean classification percentages color-coded from low (black, 0%) to high (white, 60%). We examined confusion matrices for both ethogram classification (Fig. 6*B*, left) and shuffled classification (Fig. 6*C*, right) and compared the corresponding cells in each matrix using Bonferroni-corrected t tests. Accurate classification requires two criteria: (1) correct group classification exceeds shuffled classification, and (2) incorrect group misclassification falls below shuffled classification. This pattern indicates the model is more likely than chance to make correct predictions and avoid incorrect ones. Only Control 30 rats met both criteria (Fig. 6*C*, Column 1). Control 30 rats were correctly classified 57.57% of the time, significantly above shuffled classification ($p < 0.0031$; [(0.05/16) Bonferroni's correction]). Misclassifications as Control 10 (22.74%), PAGd 30 (13.29%), and PAGd 10 (6.40%) were all significantly below shuffled levels ($p < 0.0031$). The Control 30 ethogram was sufficiently unique from the other three groups, permitting those rats to be accurately identified.

Neither Control 10 nor PAGd 30 rats were correctly classified above shuffled levels ($p > 0.0031$). Furthermore, all Control 10 misclassifications failed to fall below shuffled levels. PAGd 30 misclassifications fell below shuffled levels for comparisons to Control 30 (8.97%) and Control 10 (27.47%) but not for PAGd 10 (26.60%). PAGd 10 rats were correctly classified above shuffled levels (25.77%, $p < 0.0031$). However, PAGd 10 rats were misclassified as both PAGd 30 (29.71%) and Control 10 rats (44.39%) above shuffled levels. This means that PAGd 10 rats were more often predicted to be PAGd 30 rats or Control 10 rats than their actual group membership. Ethogram, shuffled, and differential classification means are shown in Table 2.

Confusion matrices for all rats strongly suggest that the unique behavioral profile of the Control 30 rats drives classification accuracy. In contrast, the similar behavioral profiles for Control 10, PAGd 30, and PAGd 10 rats drives confusion. To formally test this, we performed LDA with the Control 30 rats omitted. Now, overall ethogram classification accuracy (mean 37.37% across 200 models) did not statistically differ from shuffled classification accuracy (mean 35.73% across 200 models), confirmed with independent-sample t test ($t_{(398)} = 0.81$, $p = 0.42$; Fig. 6*D*). The shuffled and ethogram confusion matrices returned similar results (Fig. 6*E*). No group was correctly classified above shuffled levels (all $p > 0.005$; Fig. 6*F*), and misclassification patterns mirrored the patterns from the full analysis. LDA results reveal that PAG deletion abolishes probability-dependent scaling of fear responding, reducing high-probability rats' behavior to low-probability levels.

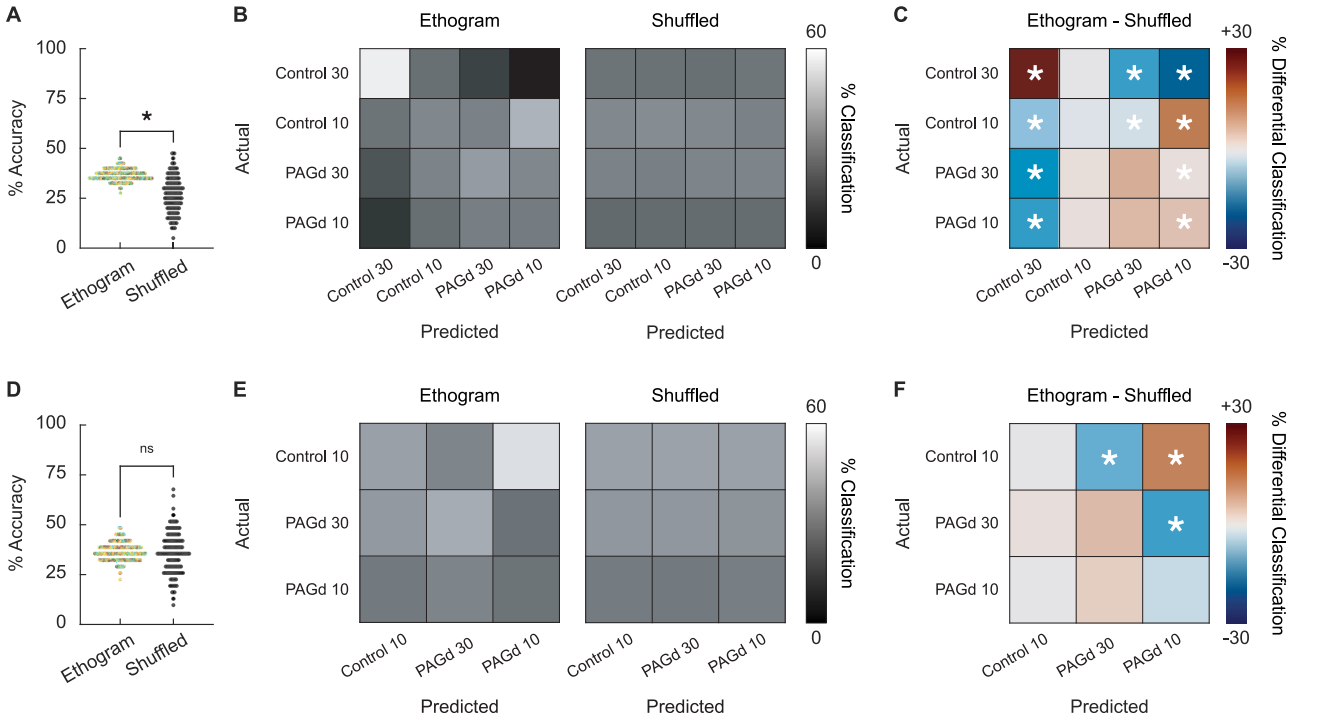


Figure 6. Ethograms and LDA. ***A***, The percentage of classification accuracy for each of the 200 LDA models is shown for the complete ethogram data (colored points) and shuffled ethogram data (black). *Significance of an independent-sample *t* test ($p < 0.05$). ***B***, Confusion matrices for the ethogram (left) and shuffled (right) datasets are shown. The predicted group label is indicated on the *x*-axis and the actual group label on the *y*-axis. Each column totals 100%, with the specific percentage of prediction visualized in each cell [0% (black) to 60% (white)]. (***C***) The percentage of differential classification (ethogram − shuffled) is shown. *Significance of an independent-sample *t* test ($p < 0.05$) comparing cell accuracy for ethogram vs shuffled data. ***D–F***, Identical plots are made for LDA classification performed for only Control 10, PAGd 30, and PAGd 10 rats.

Table 2. LDA mean classification results, Experiment 1

	Ethogram classification all rats			
Control 30%	57.57	21.27	8.97	0.13
Control 10%	22.74	29.72	27.47	44.39
Casp 30%	13.29	28.33	36.96	29.71
Casp 10%	6.40	20.68	26.60	25.77
	Control 30%	Control 10%	Casp 30%	Casp 10%
Column sum	100.00	100.00	100.00	100.00
	Shuffled classification all rats			
Control 30%	22.74	21.92	21.44	23.41
Control 10%	30.05	31.35	29.99	27.63
Casp 30%	27.94	27.00	28.73	28.74
Casp 10%	19.27	19.73	19.84	20.23
	Control 30%	Control 10%	Casp 30%	Casp 10%
Column sum	100.00	100.00	100.00	100.00
	Differential classification all rats			
Control 30%	34.82	−0.65	−12.47	−23.28
Control 10%	−7.30	−1.63	−2.52	16.76
Casp 30%	−14.66	1.33	8.23	0.98
Casp 10%	−12.86	0.95	6.77	5.54
	Control 30%	Control 10%	Casp 30%	Casp 10%
Column sum	0.00	0.00	0.00	0.00

The mean percentage of classification (actual group × predicted group) is shown for the ethogram-based, shuffled, and differential (ethogram–shuffled) linear discriminant models across Control 30, Control 10, PAGd 30, and PAGd 10 rats.

Relationships across behavioral measures

One motivation to perform this study was to probe more fundamental roles for the PAG in the rate and asymptote of fear learning in a conditioned suppression setting. A second motivation was to probe essential roles of the PAG in scaling fear responding to threat probability. Having demonstrated these roles and more, we sought to determine the nature of behavioral changes brought on by deletion. Does the PAG serve a single unified function across these behaviors or multiple distinct roles? To determine this, we assembled behavioral measures from baseline and cue periods capturing salient PAG contributions. We then examined relationships between all measures via a correlation matrix (Supplemental Fig. 3*A*). A singular role would see strong correlations between behaviors across these disparate time periods and sessions. Multiple, independent roles would be supported by observing sparse correlations. The results support multiple, independent roles. Significant ($p < 0.001$, Bonferroni-corrected for 45 comparisons), positive correlations were only found when comparing baseline nose poke rates ($r = 0.85$, $p = 4.50 \times 10^{-12}$; Supplemental Fig. 3*B*) and threat cue suppression ratios ($r = 0.88$, $p = 4.04 \times 10^{-14}$; Supplemental Fig. 3*C*) during conditioning and extinction. This shows that Control and PAGd response profiles were remarkably consistent across conditioning and extinction. A significant negative correlation was found when comparing conditioning threat cue suppression ratio and baseline locomotion ($r = 0.54$, $p = 3.50 \times 10^{-4}$). Rats showing higher threat-elicited locomotion during extinction showed lower threat cue suppression ratios during conditioning. Sparse correlations were observed when groups were examined separately (Supplemental Fig. 4).

General versus specific threat estimation roles of the PAG

The results of Experiment 1 are consistent with a role of the PAG in probability-driven scaling of fear responding. Alternatively, the Experiment 1 results may reveal a more general role in threat estimation or an essential role in footshock processing. Deleted rats could have difficulty processing surprising, error-driven footshock features (Ozawa et al., 2017; Walker et al., 2019) or

sensory/nociceptive footshock features (Samineni et al., 2017; Hu et al., 2022). In either case, probability-insensitive fear responding would be due to impairments in footshock processing.

To test these accounts, we turned to unconditioned stimulus inflation, a gold standard means of assessing rats' ability to form and update threat predictions. In the traditional design, a cue is paired with a mild footshock. Next, subjects receive a mild (control group) or intense (experimental group) footshock. Cue responding is assessed in extinction. The unconditioned stimulus inflation effect sees experimental subjects spontaneously increase cued fear responding (Rescorla, 1974). One interpretation of this result is that subjects formed a precise shock intensity prediction during initial conditioning. When the shock's intensity was inflated, subjects spontaneously updated their cued prediction, resulting in greater cue-elicited fear responding.

We sought to devise a rigorous test of rats' inflation abilities by assessing two forms: inflation through inference and inflation through direct experience (Fig. 7*A*). All rats initially received separate pairings of a 10 s tone and a 10 s light with a mild, 0.35 mA footshock. Next, experimental rats received a short session in which the 10 s light was paired with an intense, 3 mA footshock. Control rats received additional pairings of the 10 s light and the initially trained 0.35 mA footshock. All rats received an immediate tone extinction test 5 min following footshock. The critical test came 1 week later when the tone and then the light were tested during extinction. Tone responding reflected inferential inflation (the tone had never been paired with intense footshock), while light responding reflected direct inflation (the light was directly paired with intense footshock). Intact inferential and direct inflation in deleted rats would reveal a specific role of the PAG in probability-driven fear responding. Impaired inflation would suggest a more general role in threat estimation or a fundamental role in footshock processing.

Experiment 2

Forty Long–Evans rats (20 ordered from Charles River Laboratories, and 20 bred within the Boston College Animal Care Facility) received viral infusions targeting the ventrolateral PAG. The surgical approach was identical to Experiment 1, and the final rat numbers were Control rats ($n = 20$; 10 females, 10 ordered) and PAG deletion (PAGd) rats ($n = 20$; 10 females, 10 ordered). Rats in each surgical condition were then assigned to an inflation group (3 or 0.35 mA) resulting in a 2×2 design: AAV × Intensity (Fig. 7*B*).

To quantify neuron number across the anterior–posterior extent, we processed six sections per rat, spaced by ~0.5 mm,

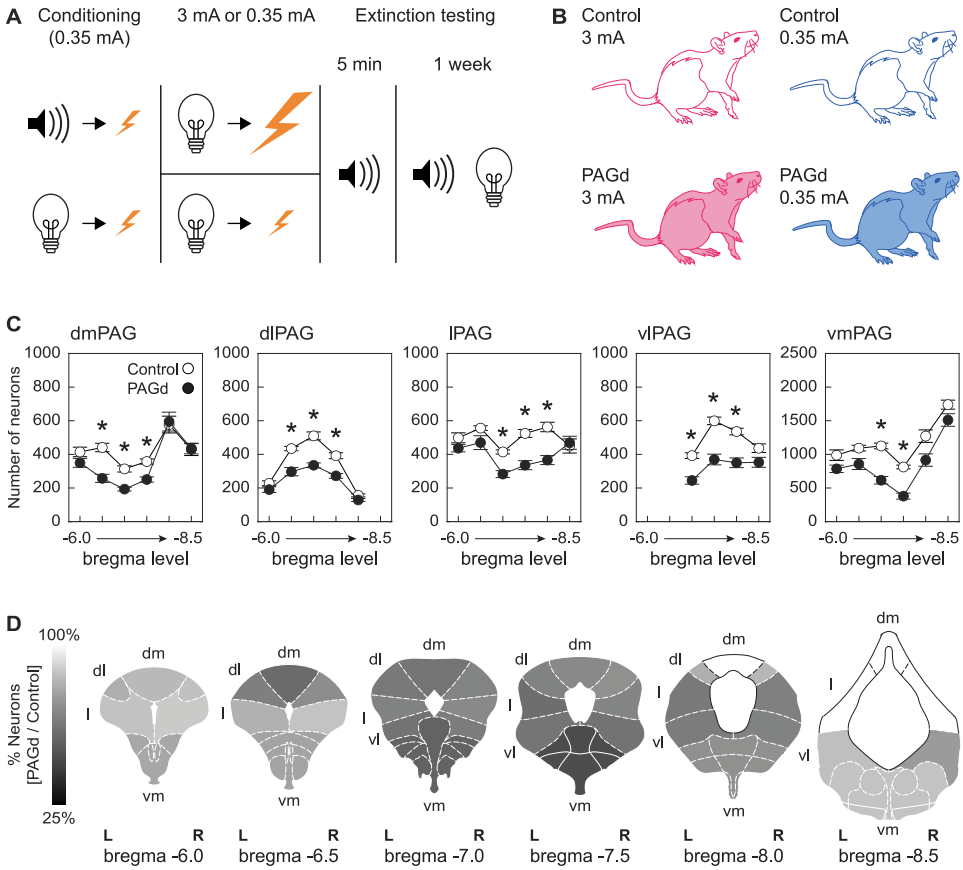


Figure 7. Experiment 2 design and histology. ***A***, All rats received fear conditioning to a light and tone with a 0.35 mA footshock and then a condensed conditioning session with light and 0.35 mA or 3 mA footshock. Tone extinction responding was assessed 5 min later. One week later, tone then light extinction responding was assessed. ***B***, The total experimental design yielded four groups defined by AAV condition and shock intensity: Control 3 mA (open magenta, top left), Control 0.35 mA (open blue, top right), PAGd 3 mA (filled magenta, bottom left), and PAGd 0.35 mA (filled blue, bottom right). ***C***, Mean ± SEM neuron number for Control (open symbols) and PAGd (closed symbols) rats is shown for five periaqueductal subregions (dmPAG, dorsomedial; dlPAG, dorsolateral; lPAG, lateral; vlPAG, ventrolateral; and vmPAG, ventromedial), across six bregma levels (−6.0, −6.5, −7.0, −7.5, −8.0, and −8.5). ***D***, The percentage of deletion is visualized as the percentage of neurons per region/bregma level in PAGd rats compared with controls. Gradient extremes are black (25% of control neuron levels) to white (100% of control neuron levels). *Significance of an independent-sample, Bonferroni-corrected *t* test.

starting at bregma −6.00 and ending at bregma −8.50. Subregion-specific and bregma-level–specific neuron counts were analyzed with ANOVA factors [AAV (Control vs PAGd), bregma level (−6.00, −6.50, −7.00, −7.50, −8.00, and −8.50), sex (female vs male), rat type (ordered vs bred), and intensity (3 vs 0.35 mA)]. The primary ANOVA results are shown in Table 3. Relative to Control rats, PAGd rats showed significant reductions in neuron number in all subregions (data in Fig. 1*C*; visualizations in Fig. 7*C*,*D*). Deletion was most pronounced between bregma levels −7.00 and −8.00 in the lateral, ventrolateral, and ventromedial subregions. Complete mappings of deletion extent are shown in Figure 2*B*. With histology confirming robust neuronal deletion, final group numbers were as follows: Control 3 mA ($n = 10$; three female-ordered, two male-ordered, two female-bred, three male-bred), Control 0.35 mA ($n = 10$; three female-ordered, two male-ordered, two female-bred, three male-bred), PAGd 3 mA ($n = 10$; three female-ordered, two male-ordered, two female-bred, three male-bred), and PAGd 0.35 mA ($n = 10$; three female-ordered, two male-ordered, two female-bred, three male-bred).

Following recovery, rats were shaped to nose poke for food pellets, and nose poking was reinforced on a variable interval 60 s schedule during each session. Baseline nose poke rates increased across the four initial sessions (2 pre-exposure→2 conditioning) and did not differ by deletion status (Fig. 8*A*,*B*). In support, ANOVA for baseline nose poke rate [between-subject factors AAV (Control vs PAGd), sex (female vs male), rat type (ordered vs bred), and intensity (3 vs 0.35 mA) and within-subject factors session (pre-exposure vs conditioning) and trial (1–6)] revealed a significant main effect of session ($F_{(1,24)} = 8.59$, $p = 0.007$). No significant main effects were found for AAV, sex, rat type, or intensity (all $p \geq 0.12$), and no significant sex interactions were found (all $p \geq 0.12$).

PAG neuronal deletion typically reduces nose poke suppression

All rats then received pre-exposure (two sessions), then conditioning (two sessions) to a 10 s visual cue and a 10 s auditory cue. Conditioning saw the cues separately predict 0.35 mA footshock. All rats showed high initial tone-elicited nose poke suppression that decreased across pre-exposure trials (Fig. 8*C*,*D*). During conditioning, tone-elicited nose poke suppression increased in both groups but more greatly in Control rats. ANOVA for tone suppression ratio [between-subjects factors AAV (Control vs PAGd), sex (female vs male), rat type (ordered vs bred), and intensity (3 vs 0.35 mA) and within-subject factors session (two pre-exposure and two conditioning) and trial (1–3)] revealed significant main effects of AAV ($F_{(1,24)} = 7.93$, $p = 0.01$), sex ($F_{(1,24)} = 5.995$, $p = 0.022$), session ($F_{(3,72)} = 42.77$, $p = 5.56 \times 10^{-6}$), and trial ($F_{(2,48)} = 3.27$, $p = 0.047$). Light-elicited nose poke suppression remained high throughout pre-exposure and conditioning in all rats (Fig. 8*E*,*F*). ANOVA for light suppression ratio (factors as for tone) revealed a significant main effect of session ($F_{(3,72)} = 14.83$, $p = 1.29 \times 10^{-7}$), trial ($F_{(2,48)} = 4.53$, $p = 0.016$), and the session trial interaction ($F_{(6,144)} = 3.62$, $p = 0.0022$), but no significant main effect of AAV ($F_{(1,24)} = 0.47$, $p = 0.50$).

During the light-shock inflation session, Control rats showed higher light-elicited nose poke suppression than PAGd rats across all five trials, with suppression remaining stable within the session for both groups (Supplemental Fig. 5). ANOVA for light suppression ratio [between-subjects factors AAV (Control vs PAGd), sex (female vs male), rat type (ordered vs bred), and intensity (3 vs 0.35 mA) and within-subjects factor trial (1–5)] revealed a significant main effect of AAV ($F_{(1,24)} = 9.68$, $p = 0.0047$). No other significant main effects or AAV interactions were observed.

During the tone extinction session administered 5 min following the end of the light-shock inflation session, both groups showed high initial tone-elicited suppression that declined across the 10 trials, consistent with within-session extinction. Control rats sustained higher suppression throughout compared with PAGd rats. ANOVA for tone suppression ratio [factors as for light, with trial (1–10)] revealed significant main effects of AAV ($F_{(1,24)} = 14.03$, $p = 0.001$), sex ($F_{(1,24)} = 5.36$, $p = 0.029$), and trial ($F_{(9,216)} = 12.31$, $p = 1.103 \times 10^{-15}$). However, baseline nose poking was strongly suppressed by the intense shock in both tests (Supplemental Fig. 5). By the end of the light inflation session, nose poke rates dropped to near zero for 3 mA rats, an effect that continued through the start of the first tone extinction session. In support, ANOVA for baseline nose poke rates revealed a significant main effect of intensity during the light-shock inflation session ($F_{(1,24)} = 60.045$, $p = 5.52 \times 10^{-8}$) and significant intensity × trial interactions for both the light-shock inflation session ($F_{4,96} = 6.00$, $p = 2.38 \times 10^{-4}$) and the tone extinction session ($F_{(1,24)} = 8.07$, $p = 2.73 \times 10^{-10}$). This means that suppression ratio, which uses baseline nose poke rate as a factor, is not a reliable indicator of responding during the first tone extinction test.

PAG neuronal deletion leaves inferred and constrains direct inflation

The critical test of inferential inflation came 1 week following the light-shock inflation session, when the tone was again presented in extinction. As during the prior extinction test, PAGd rats showed reduced tone responding compared with Control rats. In contrast to the prior test, inferential inflation was evident. Rats that had light paired with the 3 mA footshock a week prior showed elevated tone-evoked fear responding compared with rats that had light paired with the 0.35 mA footshock (Fig. 9*A*,*B*). In support, ANOVA for tone suppression ratio [between-subject factors AAV (Control vs PAGd), sex (female vs male), rat type (ordered vs bred), and intensity (3 vs 0.35 mA) and within-subjects factor trial (1–10)] revealed significant main effects of AAV ($F_{(1,24)} =$

Table 3. ANOVA results for neuron number quantification, Experiment 2

PAG subregion	AAV main effect		Bregma main effect		AAV × bregma interaction	
Dorsal	**$F_{(1,32)} = 9.045$**	***p = 0.0051***	**$F_{(5,160)} = 38.25$**	***$p = 1.07 \times 10^{-25}$***	**$F_{(5,160)} = 3.907$**	***p = 0.0023***
Dorsolateral	**$F_{(1,32)} = 76.4$**	***$p = 5.48 \times 10^{-10}$***	**$F_{(4,128)} = 214.4$**	***$p = 1.06 \times 10^{-55}$***	**$F_{(4,12)8} = 16.32$**	***$p = 7.891 \times 10^{-11}$***
Lateral	**$F_{(1,32)} = 37.72$**	**$p = 7.21 \times 10^{-7}$**	**$F_{(5,160)} = 13.88$**	**$p = 2.91 \times 10^{-11}$**	**$F_{(5,160)} = 7.964$**	**$p = 1.002 \times 10^{-6}$**
Ventrolateral	**$F_{(1,32)} = 76.88$**	**$p = 5.10 \times 10^{-10}$**	**$F_{(3,96)} = 37.59$**	**$p = 3.74 \times 10^{-16}$**	**$F_{(3,96)} = 6.586$**	**$p = 4.28 \times 10^{-4}$**
Ventral	**$F_{(1,32)} = 35.49$**	***$p = 1.23 \times 10^{-6}$***	**$F_{(5,16)0} = 67.04$**	***$p = 1.73 \times 10^{-37}$***	**$F_{(5,160)} = 2.17$**	*p = 0.0601*

F and *p* values are shown for the main effects of AAV (Control vs PAGd) and bregma level and their interaction on neuron number within each PAG subregion (dorsal, dorsolateral, lateral, ventrolateral, ventromedial). Bold indicates ANOVA significance.

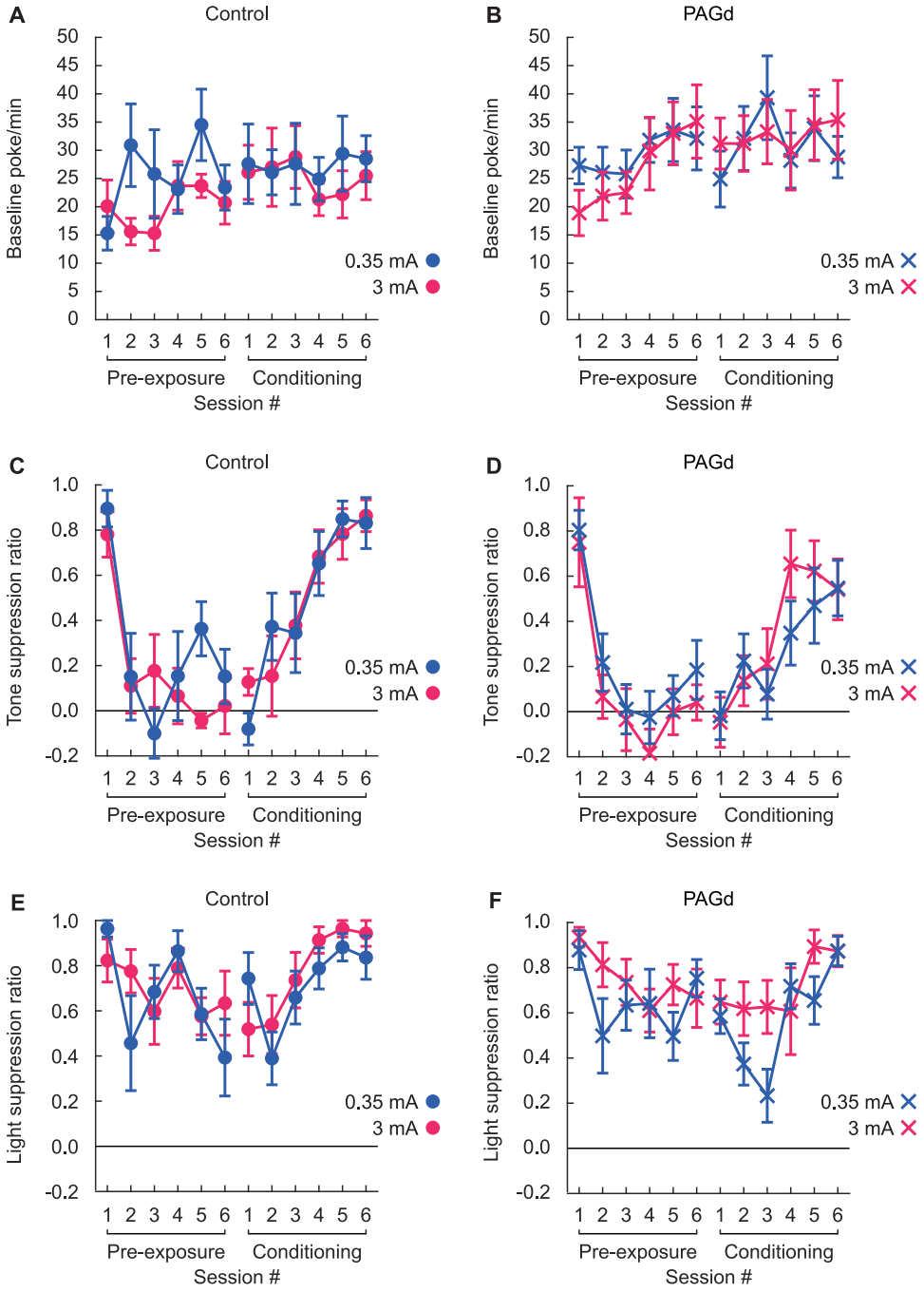


Figure 8. Responding during pre-exposure and conditioning. Mean ± SEM baseline nose poke rate (poke/minute) is shown for (***A***) Control rats and (***B***) PAGd rats assigned to 0.35 mA (blue) or 3 mA (magenta) footshock across the trials of pre-exposure and conditioning. Mean ± SEM tone suppression ratio is shown for (***C***) Control rats and (***D***) PAGd rats across pre-exposure and conditioning. Mean ± SEM light suppression ratio is shown for (***E***) Control rats and (***F***) PAGd rats across pre-exposure and conditioning.

6.72, $p = 0.016$), intensity ($F_{(1,24)} = 11.96$, $p = 0.002$), and trial ($F_{(9,216)} = 14.60$, $p = 2.22 \times 10^{-18}$). Independent-sample t test for 3 vs 0.35 mA rats (Controls and PAGd combined) revealed significant suppression ratio differences ($t_{(38)} = 2.86$, $p = 0.007$). Separate t tests revealed no significance for Control rats ($t_{(18)} = 1.54$, $p = 0.14$), significance for PAGd rats ($t_{(18)} = 3.79$, $p = 0.0013$), but no significant difference between the Control and PAGd patterns ($t_{(18)} = 0.33$, $p = 0.75$).

The critical test of direct inflation came when the light was presented in extinction. Direct inflation was evident in both groups. Light-elicited nose poke suppression remained near ceiling across the five light extinction trials for Control and PAGd 3 mA rats. In contrast, Control and PAGd 0.35 mA rats showed lower light-elicited nose poke suppression that further decreased as trials progressed (Fig. 9*C*,*D*). Low light-elicited nose poke suppression was particularly prominent in PAGd 0.35 mA rats. In support, ANOVA for light suppression ratio [factors as for tone, with trial (1–5)] revealed significant main effects of intensity ($F_{(1,24)} = 26.72$, $p = 2.71 \times 10^{-5}$) and AAV ($F_{(1,24)} = 5.66$, $p = 0.026$). Independent-sample t test for 3 versus 0.35 mA rats (Controls and PAGd combined) revealed significant suppression ratio differences ($t_{(38)} = 5.38$, $p = 4.10 \times 10^{-6}$). Separate t tests revealed significance for Control rats ($t_{(18)} = 3.12$, $p = 0.006$), as well as significance for PAGd rats ($t_{(18)} = 5.22$, $p = 5.83 \times 10^{-5}$).

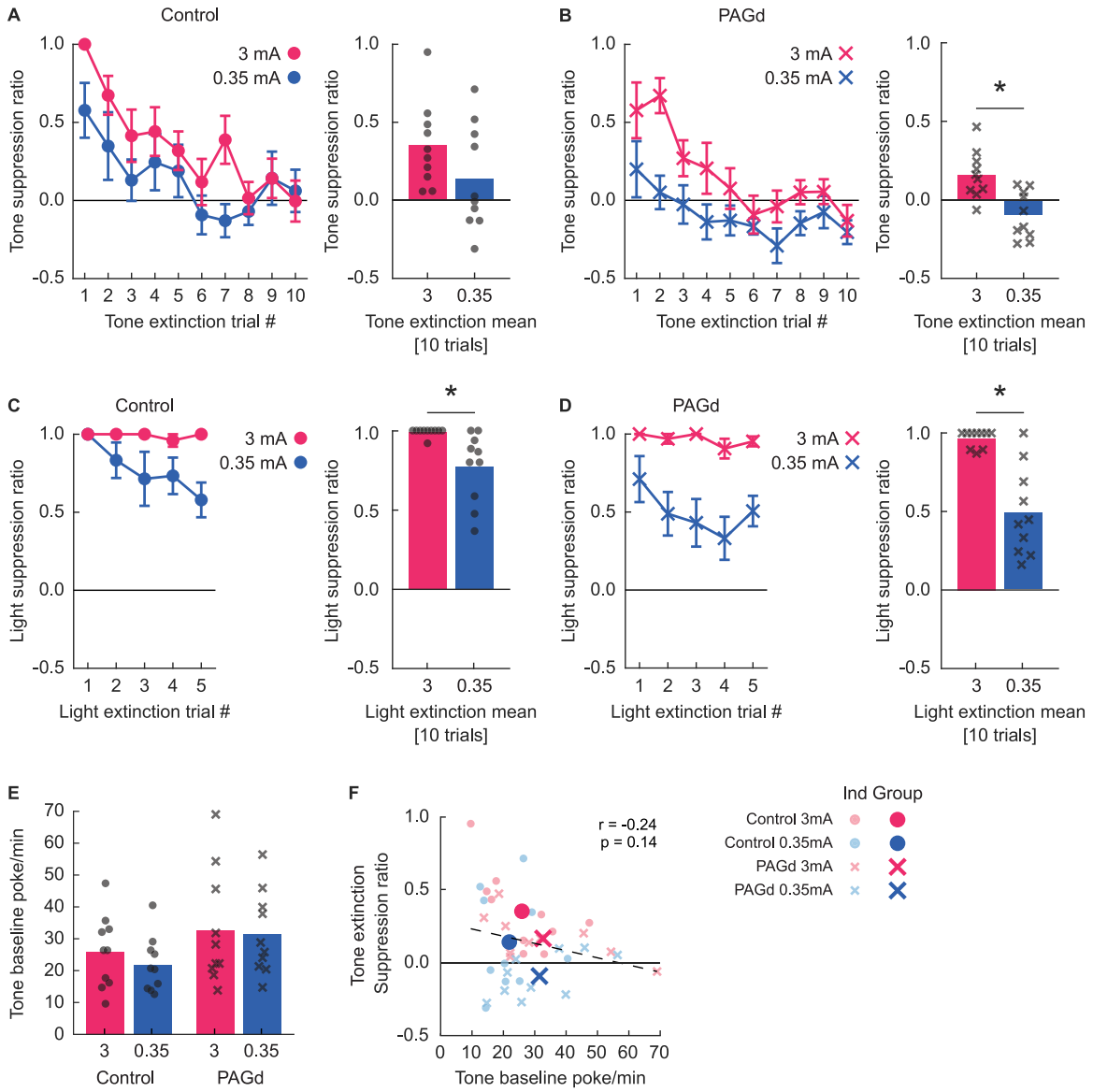


Figure 9. Responding during extinction 1 week after light-shock inflation. Mean ± SEM tone suppression ratio (left) and group (bar) and individual (symbols) mean tone suppression ratio for all 10 trials (right) are shown for (***A***) Control rats and (***B***) PAGd rats assigned to 3 mA (magenta) or 0.35 mA (blue) footshock across the 10 tone extinction trials. Mean ± SEM light suppression ratio (left) and group (bar) and individual (symbols) mean light suppression ratio for all five trials (right) are shown for (***C***) Control rats and (***D***) PAGd rats across the five light extinction trials. *(***A–D***) significance of an independent-sample *t* test ($p < 0.05$). (***E***) Group (bar) and individual (circles and Xs) mean tone baseline nose poke rate is shown for Control and PAGd rats. ***F***, Scatterplot compares group (large, opaque symbols) and individual (small, transparent symbols) tone baseline nose poke rate (*x*-axis) versus tone suppression ratio (*y*-axis) during the tone extinction test, coded by AAV (circle = Control, X = PAGd) and intensity (magenta = 3 mA, blue = 0.35 mA); the dotted line indicates linear trend across all rats.

Only now there was a significant difference between the Control and PAGd pattern ($t_{(18)} = 2.25$, $p = 0.037$). The direct inflation effect was larger in PAGd rats.

Equivalent demonstration of inferred unconditioned stimulus inflation in Control and PAGd rats was accompanied by equivalent baseline nose poke responding (Fig. 9*E*). In support, ANOVA for baseline nose poke rate during the tone extinction session [factors as above, with trial (1–10)] revealed no significant main effect of AAV ($F_{(1,24)} = 2.37$, $p = 0.14$). Furthermore, baseline nose poke rates and cue suppression ratios were not correlated during the tone test ($r = -0.24$, $p = 0.14$; Fig. 9*F*).

Ethograms reveal unique behavioral profiles for PAG neuronal deletion and unconditioned stimulus inflation

In an effort to reveal the behavioral underpinnings of neuronal deletion and unconditioned stimulus inflation, we constructed comprehensive, high-temporal-resolution ethograms from video taken during the final tone extinction test. Complete ethograms are shown for each group (Fig. 10*A–D*). The ethograms show three prominent patterns. PAG neuronal deletion dramatically reduced freezing. Unconditioned stimulus inflation altered the total time course of nose poking (precue through cue and post). Unique, multibehavior patterns reflected neuronal deletion versus unconditioned stimulus inflation during the cue period.

We first analyzed the four most dominant behaviors in both Experiments 1 and 2 (poke, cup, freeze, and rear) with repeated-measure ANOVA across the full trial [between-subject factors AAV (Control vs PAGd), intensity (3 vs 0.35 mA), sex (female vs male), and rat type (ordered vs bred); within-subject factor time (100, 200 ms intervals)]. Neuronal deletion reduced freezing across the trial, while shock intensity shaped the time course of poking. In support, freezing showed a main effect of AAV

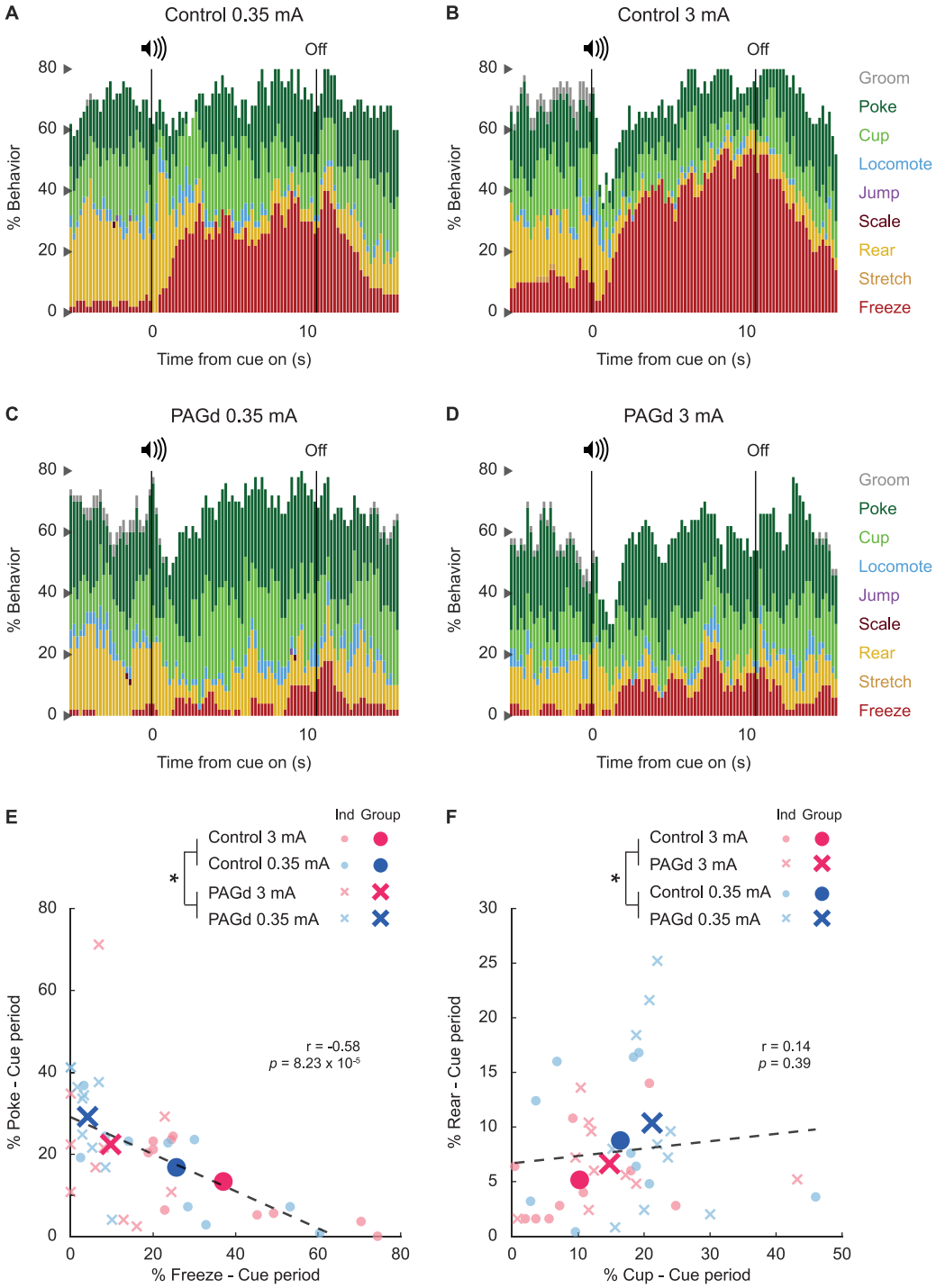


Figure 10. Ethograms. The mean percentage of behavior (*y*-axis) before, during, and after the cue period (*x*-axis) is shown for (***A***) Control 3 mA, (***B***) Control 0.35 mA, (***C***) PAGd 0.35 mA, and (***D***) PAGd 3 mA rats. The behaviors included (gray) groom, (dark green) poke, (light green) cup, (light blue) locomotion, (purple) jump, (maroon) scale, (yellow) rear, (orange) stretch, and (red) freeze. ***E***, Scatterplot compares group (large, opaque symbols) and individual (small, transparent symbols) percentage of freezing (*x*-axis) versus percentage of poking (*y*-axis) during the cue period for Control 3 mA, Control 0.35 mA, PAGd 3 mA, and PAGd 0.35 mA rats. *Significance of an independent-sample *t* test ($p < 0.05$). ***F***, The same comparison is plotted for the percentage of cupping (*x*-axis) versus the percentage of rearing (*y*-axis) during the cue period.

($F_{(1,24)} = 25.18$, $p = 3.97 \times 10^{-5}$) and an AAV × time interaction ($F_{(99,2376)} = 4.50$, $p = 1.80 \times 10^{-40}$). Poking showed an intensity × time interaction ($F_{(99,2376)} = 1.41$, $p = 0.005$). Restricting analysis to the cue period revealed partial, differential behavioral bases for shock intensity and deletion status. The ethogram behaviors, cup (intensity $F_{(1,24)} = 6.54$ vs AAV, $F_{(1,24)} = 1.16$) and rear (intensity $F_{(1,24)} = 2.66$ vs AAV, $F_{(1,24)} = 0.53$), had larger main effect *F* statistics for intensity, compared with deletion status. In contrast, freeze (AAV $F_{(1,24)} = 25.08$ vs intensity $F_{(1,24)} = 3.66$) and poke (AAV $F_{(1,24)} = 3.48$ vs intensity $F_{(1,24)} = 0.46$) had larger main effect *F* statistics for deletion status, compared with intensity. We therefore used Hotelling's T^2 to test the joint freezing and poking profile for an effect of neuronal deletion and the joint cup and rearing profile for an effect of shock intensity.

Hotelling's T^2 test for the combined freezing and poking profile confirmed significant multivariate separation based on

deletion status ($T^2 = 21.46$, equivalent $F_{(2,37)} = 10.45$, $p = 2.53 \times 10^{-4}$). Control rats froze more and poked less (freezing = 29.60%, poking = 16.71%), while PAGd rats froze less and poked more (freezing = 6.97%, poking = 25.48%). Across all rats, cue period freezing and poking were negatively correlated (Fig. 10*E*; $r = -0.58$, $p = 8.23 \times 10^{-5}$). Hotelling's T^2 test for the combined cup and rearing profile confirmed significant multivariate separation based on unconditioned stimulus inflation status ($T^2 = 6.91$, equivalent $F_{(2,37)} = 3.36$, $p = 0.046$). Rats receiving the intense, 3 mA footshock showed less cup and rearing (cup = 12.88%, rearing = 6.71%) than rats receiving the mild, 0.35 mA footshock (cup = 18.56%, rearing = 10.08%). Cup and rearing showed zero correlation across rats (Fig. 10*F*; $r = 0.14$, $p = 0.39$).

Discussion

The prevailing view of the brain's fear circuit sees threat predictions generated by the amygdala sent to the PAG to elicit freezing. We assessed intact and PAG-deleted rats in two fear conditioning settings. Probabilistic fear discrimination required rats to form and use precise threat probability predictions to scale fear responding. Unconditioned stimulus inflation required rats to form and update precise shock intensity predictions to increase fear responding via inference or direct experience. In both settings, freezing was one component of a suite of behaviors orchestrated by the threat cue. In surface-level support of the prevailing view, PAG deletion reduced freezing in both settings.

Yet, losing the PAG did not simply mean losing freezing. During probabilistic fear discrimination, losing the PAG meant losing the ability to scale the total suite of fear responding to threat probability. Rats lacking their PAG responded to a high-threat cue as if it were a low-threat. During unconditioned stimulus inflation, losing the PAG meant markedly reduced freezing. Yet, these same rats retained the ability to form and update threat predictions based on shock intensity. This included updating that was based on inference and direct experience. This pattern of results cannot be explained by a serial pathway that sees the PAG's sole role as that of a freezing elicitor. The PAG is essential to form/use precise predictions to scale behavior to threat probability and boost fear responding to higher probability threats. The unconditioned stimulus inflation results further show that impairments in probability-dependent fear scaling were not due to deficits in footshock processing, as demonstrating inflation required precise footshock intensity information.

Before discussing our findings more broadly, some caveats and considerations are noted. First, the dual-viral approach (Russell and McDannald, 2024; Moaddab et al., 2025) meant that neurons were deleted prior to all conditioning and testing. The present results cannot distinguish between PAG contributions to learning versus expression. Second, the deletions were pan-neuronal. Our results cannot conclusively ascribe control of probability-dependent scaling of fear responding to a specific genetic/projection type (although we speculate on possible identities below).

Third, we observed neuronal deletion outside of the lateral and ventrolateral PAG. This was expected. Given that no prior role in scaling fear responding to threat probability had been demonstrated, we planned for a deletion with high penetrance. The 2.5+ mm anterior–posterior span of the periaqueductal columns means that achieving high penetrance would necessitate lesser specificity to the ventrolateral and lateral columns. If there had been no impact of a high-penetrance deletion on probability-dependent responding, a negative finding would have been meaningful. In contrast, optimizing deletion for specificity would necessitate lesser penetrance. In this case, a negative finding would be inconclusive as it could be explained by an incomplete deletion. Our observed deletion included cell loss in the "ventromedial" PAG. We use this term loosely, as the regions comprising the ventromedial PAG shift substantially going from oculomotor nuclei (anterior) to dorsal raphe (mid) to laterodorsal tegmental nuclei (posterior). While we cannot totally rule out cell loss in these regions leading to deficits, we have shown that complete deletion of dorsal raphe serotonin neurons leaves acquisition and expression of probabilistic fear discrimination intact (Walker et al., 2022). Furthermore, the majority of the laterodorsal tegmental nucleus is posterior to our deletion area.

The Experiment 1 results are consistent with the view of the PAG as the source of a positive, aversive prediction error that functions to strengthen cue–shock associations and facilitate cue-elicited defensive responding (Ozawa et al., 2017; Walker et al., 2019). As the result of losing the PAG, learning proceeded more slowly, and the final levels of threat cue responding were diminished. Of course, learning was not altogether abolished. This indicates that there are additional neural sources of prediction error or that learning can be achieved through alternative error mechanisms (Yau and McNally, 2019).

The Experiment 1 results further reveal the PAG to at least be the organizer of a more sophisticated behavioral output than freezing. Baseline behavior in our fear discrimination setting is a mix of rearing (exploratory), food cup checking and nose poking (reward), and freezing (defensive). Losing the PAG sees this baseline become skewed away from defensive behavior and toward exploration and reward seeking. When threat cues are presented, the most noticeable impact of PAG deletion is on the initial cue responding when shock is most distal. This is perhaps surprising given the opposing pattern seen in human threat settings (Mobbs et al., 2007) but is consistent with rapid probability signaling in rodents (Wright and McDannald, 2019). As footshock drew near, the total behavior pattern of intact and deleted rats converged. This pattern reveals that deletion did not totally impair behavioral responding and that, in this setting, the PAG is primarily organizing distal aspects of behavior systems-level responding.

Although this experiment cannot link genetic/projection-specific cell types to specific functions, PAG cell-type composition and its relation to fear output have been examined in considerable detail. Ventrolateral PAG glutamatergic ($VGluT2^+$) neurons have low baseline firing rates and are necessary/sufficient to produce freezing through direct projections to the magnocellular reticular nucleus (Tovote et al., 2016). GABAergic neurons have high baseline firing rates, responding to threat cues with inhibition. We previously recorded single units in caudal vlPAG during graded-probability fear discrimination (Wright and McDannald, 2019). The short-latency signal that best tracked shock probability, independent of fear output, was carried exclusively by low-firing-rate neurons through increases in firing, a class comparable to the $VGluT2^+$ population. Two scenarios seem most likely. One, periaqueductal signals for threat probability are found in $VGluT2^+$ neurons while signals for behavior are found in GABAergic neurons. Two, $VGluT2^+$ populations with distinct projection profiles signal freezing, prediction error, and threat probability. So while $VGluT2^+$ neurons projecting to the reticular nucleus may mediate freezing, parabrachial nucleus (Pyeon et al., 2025) projecting neurons may signal threat probability (Campos et al., 2018), and

central amygdala projecting neurons may signal prediction error (Xie et al., 2025).

The Experiment 2 results work to specify PAG roles in the two settings examined. First, just as in the probabilistic setting, the PAG influenced the baseline balance of reward-related responding and freezing. Losing the PAG meant reduced baseline freezing, enhanced baseline reward seeking, and lesser suppression of reward seeking. Despite this, losing the PAG not only left inferential inflation intact but actually permitted greater expression of direct inflation. This was driven by the mild intensity condition, with deleted rats showing greater reductions in fear responding compared with their control counterparts.

What does this mean for the neural basis of unconditioned stimulus inflation and for the role of the PAG in the fear circuit? First, the neural basis of unconditioned stimulus inflation remains a mystery. Our finding of no role of the PAG joins two prior studies finding no role of the basolateral amygdala (Rabinak and Maren, 2008; Rabinak et al., 2009). Two of the three main nodes in the fear circuit are dispensable for unconditioned stimulus inflation. Either the critical node has not yet been identified (perhaps the central amygdala or prelimbic cortex) or unconditioned stimulus inflation is normally the product of multiple behavioral processes, each using separate neural circuits.

As for the role of the PAG in the fear circuit, our combined results still suggest function focused on organizing defensive behavior. Yet, defensive behavior is not as simple as turning freezing on and off. Organizing a complete and appropriate response first means modulating the baseline engagement of multiple behavior systems (reward, exploration, defensive, and more). These behavioral systems must further be modulated and balanced proportionally to the current degree of threat. When rats are placed in minimally engaging contexts characterized by intense footshock, the PAG will function to organize the appropriate behavior: freezing. However, when rats are placed in richer contexts featuring a mix of rewarding and threatening outcomes—and further with those threatening outcomes coming in a range of probabilities—the PAG will still function to organize behavior. Only now organizing behavior requires multiple systems to be modulated with respect to context valences, time to threat, threat probability, and additional relevant factors.

One motivation to focus on amygdala and frontal cortex (dys) function in disordered anxiety is their central role in threat estimation. Here we show that the PAG is not simply a relay that converts a threat estimate into freezing. The PAG shifts the balance of defensive, exploratory, and reward-related behavior systems with respect to threat probability, context, and time. These results give the PAG a more central role in the fear circuit. This positions the PAG, together with the amygdala and frontal cortex, as a site of disrupted threat estimation in disordered anxiety (George et al., 2019).

References

Amorapanth P, Nader K, LeDoux JE (1999) Lesions of periaqueductal gray dissociate-conditioned freezing from conditioned suppression behavior in rats. Learn Mem 6:491–499.

Assareh N, Sarrami M, Carrive P, McNally GP (2016) The organization of defensive behavior elicited by optogenetic excitation of rat lateral or ventrolateral periaqueductal gray. Behav Neurosci 130:406–414.

Berg S, et al. (2019) Ilastik: interactive machine learning for (bio)image analysis. Nat Methods 16:1226–1232.

Campos CA, Bowen AJ, Roman CW, Palmiter RD (2018) Encoding of danger by parabrachial CGRP neurons. Nature 555:617.

Choi J-S, Brown TH (2003) Central amygdala lesions block ultrasonic vocalization and freezing as conditional but not unconditional responses. J Neurosci 23:8713–8721.

Chu A, Gordon NT, DuBois AM, Michel CB, Hanrahan KE, Williams DC, Anzellotti S, McDannald MA (2024) A fear conditioned cue orchestrates a suite of behaviors in rats (Hill MN, Wassum KM, Maren S, eds). Elife 13: e82497.

Ciocchi S, et al. (2010) Encoding of conditioned fear in central amygdala inhibitory circuits. Nature 468:277–282.

Davis M (1992) The role of the amygdala in fear and anxiety. Annu Rev Neurosci 15:353–375.

De Oca BM, DeCola JP, Maren S, Fanselow MS (1998) Distinct regions of the periaqueductal gray are involved in the acquisition and expression of defensive responses. J Neurosci 18:3426–3432.

Estes KW, Skinner BF (1941) Some quantitative properties of anxiety. J Exp Psychol 29:390–400.

Fanselow MS, Decola JP, De Oca BM, Landeira-Fernandez J (1995) Ventral and dorsolateral regions of the midbrain periaqueductal gray (PAG) control different stages of defensive behavior: dorsolateral PAG lesions enhance the defensive freezing produced by massed and immediate shock. Aggress Behav 21:63–77.

Fanselow MS, Kim JJ (1994) Acquisition of contextual Pavlovian fear conditioning is blocked by application of an nmda receptor antagonist D, L-2-amino-5-phosphonovaleric acid to the basolateral amygdala. Behav Neurosci 108:210–212.

George DT, Ameli R, Koob GF (2019) Periaqueductal gray sheds light on dark areas of psychopathology. Trends Neurosci 42:349. Available at: https://www.ncbi.nlm.nih.gov/pubmed/30955857

Goosens KA, Maren S (2001) Contextual and auditory fear conditioning are mediated by the lateral, basal, and central amygdaloid nuclei in rats. Learn Mem 8:148–155.

Hu Z, et al. (2022) A visual circuit related to the periaqueductal gray area for the antinociceptive effects of bright light treatment. Neuron 110:1712–1727.e7.

Johansen JP, Tarpley JW, LeDoux JE, Blair HT (2010) Neural substrates for expectation-modulated fear learning in the amygdala and periaqueductal gray. Nat Neurosci 13:979–986.

Kim JJ, Rison RA, Fanselow MS (1993) Effects of amygdala, hippocampus, and periaqueductal gray lesions on short-term and long-term contextual fear. Behav Neurosci 107:1093–1098. lesions of basolateral and central nuclei of the amygdala produce differential effects on fear conditioning. J Neurosci 24:7654–7662.

Koo JW, Han JS, Kim JJ. Selective neurotoxic lesions of basolateral and central nuclei of the amygdala produce differential effects on fear conditioning. J Neurosci 24:7654–7662.

LeDoux JE, Cicchetti P, Xagoraris A, Romanski LM (1990) The lateral amygdaloid nucleus: sensory interface of the amygdala in fear conditioning. J Neurosci 10:1062–1069.

Lee JLC, Dickinson A, Everitt BJ (2005) Conditioned suppression and freezing as measures of aversive Pavlovian conditioning: effects of discrete amygdala lesions and overtraining. Behav Brain Res 159:221–233.

Li H, Penzo MA, Taniguchi H, Kopec CD, Huang ZJ, Li B (2013) Experience-dependent modification of a central amygdala fear circuit. Nat Neurosci 16:332–339.

Liu J, Totty MS, Melissari L, Bayer H, Maren S (2022) Convergent coding of recent and remote fear memory in the basolateral amygdala. Biol Psychiatry 91:832–840.

Maren S (1999) Neurotoxic basolateral amygdala lesions impair learning and memory but not the performance of conditional fear in rats. J Neurosci 19: 8696–8703.

McDannald MA (2010) Contributions of the amygdala central nucleus and ventrolateral periaqueductal gray to freezing and instrumental suppression in Pavlovian fear conditioning. Behav Brain Res 211: 111–117.

McDannald MA (2023) Pavlovian fear conditioning is more than you think it is. J Neurosci 43:8079–8087.

McNally GP, Johansen JP, Blair HT (2011) Placing prediction into the fear circuit. Trends Neurosci 34:283–292.

Moaddab M, Qian S, Boyce JB, Gordon NT, DuBois AM, Fitzpatrick AC, Zheng K, McDannald MA (2025) Paraventricular thalamic inputs to the ventral pallidum shape reward seeking during threat and fear responding in extinction. Behav Neurosci 139:255–266.

Mobbs D, Petrovic P, Marchant JL, Hassabis D, Weiskopf N, Seymour B, Dolan RJ, Frith CD (2007) When fear is near: threat imminence elicits prefrontal-periaqueductal gray shifts in humans. Science 317: 1079–1083.

Nikbakht N, Diamond ME (2021) Conserved visual capacity of rats under red light (Gold JI, Vinck M, Steinmetz N, Franke K, eds). Elife 10:e66429.

Ozawa T, Ycu EA, Kumar A, Yeh LF, Ahmed T, Koivumaa J, Johansen JP (2017) A feedback neural circuit for calibrating aversive memory strength. Nat Neurosci 20:90–97.

Pyeon GH, Cho H, Chung BM, Choi J-S, Jo YS (2025) Parabrachial CGRP neurons modulate active defensive behavior under a naturalistic threat. Elife 14:e101523.

Rabinak CA, Orsini CA, Zimmerman JM, Maren S (2009) The amygdala is not necessary for unconditioned stimulus inflation after Pavlovian fear conditioning in rats. Learn Mem 16:645–654.

Rabinak CA, Maren S (2008) Associative structure of fear memory after basolateral amygdala lesions in rats. Behav Neurosci 122:1284–1294.

Rescorla RA (1968) Probability of shock in the presence and absence of CS in fear conditioning. J Comp Physiol Psychol 66:1–5.

Rescorla RA (1974) Effect of inflation of the unconditioned stimulus value following conditioning. J Comp Physiol Psychol 86:101–106.

Russell EL, McDannald MA (2024) Ventral pallidum neurons are necessary to generalize and express fear-related responding in a minimal threat setting. eNeuro 11:ENEURO.0124-24.2024.

Samineni VK, Grajales-Reyes JG, Copits BA, O'Brien DE, Trigg SL, Gomez AM, Bruchas MR, Gereau RW (2017) Divergent modulation of nociception by glutamatergic and GABAergic neuronal subpopulations in the periaqueductal gray. eNeuro 4:ENEURO.0129-16.2017.

Signoret-Genest J, Schukraft N, Reis S L, Segebarth D, Deisseroth K, Tovote P (2023) Integrated cardio-behavioral responses to threat define defensive states. Nat Neurosci 26:447–457.

Strickland JA, McDannald MA (2022) Brainstem networks construct threat probability and prediction error from neuronal building blocks. Nat Commun 13:6192.

Tervo DGR, et al. (2016) A designer AAV variant permits efficient retrograde access to projection neurons. Neuron 92:372–382.

Tovote P, et al. (2016) Midbrain circuits for defensive behaviour. Nature 534: 206–212.

Vaaga CE, Brown ST, Raman IM (2020) Cerebellar modulation of synaptic input to freezing-related neurons in the periaqueductal gray (Aldrich RW, Kauer JA, Kauer JA, Tovote P, eds). Elife 9:e54302.

Walker RA, Wright KM, Jhou TC, McDannald MA (2019) The ventrolateral periaqueductal gray updates fear via positive prediction error. Eur J Neurosci. Available at: https://www.ncbi.nlm.nih.gov/pubmed/31376295

Walker RA, Suthard RL, Perison TN, Sheehan NM, Dwyer CC, Lee JK, Enabulele EK, Ray MH, McDannald MA (2022) Dorsal raphe 5-HT neurons utilize, but do not generate, negative aversive prediction errors. eNeuro 9:ENEURO.0132-21.2022.

Wilensky AE, Schafe GE, Kristensen MP, LeDoux JE (2006) Rethinking the fear circuit: the central nucleus of the amygdala is required for the acquisition, consolidation, and expression of Pavlovian fear conditioning. J Neurosci 26:12387–12396.

Williams DC, et al. (2025) Ethograms predict visual fear conditioning status in rats. Elife 14:e102782.

Wright KM, McDannald MA (2019) Ventrolateral periaqueductal gray neurons prioritize threat probability over fear output. Elife 8:e45013.

Xie T, et al. (2025) An excitatory circuit in the ventrolateral periaqueductal gray drives hypometabolic state during acute systemic inflammation. Cell Rep 44.

Yang CF, Chiang MC, Gray DC, Prabhakaran M, Alvarado M, Juntti SA, Unger EK, Wells JA, Shah NM (2013) Sexually dimorphic neurons in the ventromedial hypothalamus govern mating in both sexes and aggression in males. Cell 153:896–909.

Yau JO-Y, McNally GP (2019) Rules for aversive learning and decision-making. Curr Opin Behav Sci 26:1–8.